Natural Resources Research, Vol. 30, No. 3, June 2021 (© 2021)
https://doi.org/10.1007/s11053-021-09823-7

Original Paper

Predicting Ground Vibrations Due to Mine Blasting Using a Novel Artificial Neural Network-Based Cuckoo Search Optimization

Xuan-Nam Bui,[1,2] Hoang Nguyen,[1,2,5] Quang-Hieu Tran,[1,2] Dinh-An Nguyen,[1] and Hoang-Bac Bui[3,4]

Received 18 September 2020; accepted 18 January 2021
Published online: 12 February 2021

Blasting plays a fundamental role in rock fragmentation, and it is the first preparatory stage in the mining extraction process. However, its undesirable effects, mostly ground vibration, can cause severe damages to the surroundings, such as cracks/collapses of buildings, instability of slopes, deformation of underground space, affect underground water, to name a few. Therefore, the primary purpose of this study was to predict the intensity of ground vibration induced by mine blasting operations with high accuracy, aiming to reduce the severe damages to the surroundings. A novel artificial neural network (ANN)-based cuckoo search optimization (CSO), named as CSO–ANN model, was proposed for this aim based on 118 blasting events that were collected at a quarry mine in Vietnam. Besides, stand-alone models, such as ANN, support vector machine (SVM), tree-based ensembles, and two empirical equations (i.e., USBM and Ambraseys), were considered and developed for comparative evaluation of the performance of the proposed CSO–ANN model. Afterwards, they were tested and validated based on three blasting events in practical engineering. The results revealed that the CSO algorithm significantly improved the performance of the ANN model. In addition, the comparative results showed that the accuracy of the proposed hybrid CSO–ANN model was superior to the other models with MAE (mean absolute error) of 0.178, RMSE (root-mean-squared error) of 0.246, R^2 (square of the correlation coefficient) of 0.990, VAF (variance accounted for) of 98.668, and a20-index of 1.0. Meanwhile, the other models only yielded performances in the range of 0.257–0.652 for RMSE, 0.932–0.987 for R^2, 20.942–98.542 for VAF and 0.227–0.955 for a20-index. The findings also indicated that explosive charge per borehole has a special relationship with ground vibration intensity. It should be considered and used instead of total explosive charge per blast in some cases, especially for the empirical models.

KEY WORDS: Ground vibration, Blasting, Open-pit mine, Cuckoo search optimization, Deep learning.

[1]Department of Surface Mining, Mining Faculty, Hanoi University of Mining and Geology, 18 Vien Street, Duc Thang Ward, Bac Tu Liem District, Hanoi 100000, Vietnam.
[2]Center for Mining, Electro-Mechanical Research, Hanoi University of Mining and Geology, 18 Vien Street, Duc Thang ward, Bac Tu Liem District, Hanoi 100000, Vietnam.
[3]Faculty of Geosciences and Geoengineering, Hanoi University of Mining and Geology, 18 Vien Street, Duc Thang Ward, Bac Tu Liem District, Hanoi 100000, Vietnam.
[4]Center for Excellence in Analysis and Experiment, Hanoi University of Mining and Geology, 18 Vien Street, Duc Thang ward, Bac Tu Liem District, Hanoi 100000, Vietnam.
[5]To whom correspondence should be addressed; e-mail: nguyenhoang@humg.edu.vn

INTRODUCTION

Over the past several decades, blasting was introduced as the most common method for fragmenting rock mass or ore in opencast mines because of its advantages in terms of economic and technical. Its aim is to fragment intact rocks into smaller pieces to accommodate subsequent handling operations, such as loading/unloading, transporting (e.g., trucks or conveyer), dumping, and crushing. However, due to the high demand for construction materials and metals, the rapidly expanding production of open-pit mines with large amounts of explosive used is significantly rising as well (Oliveira et al. 2017). This problem leads to a variety of environmental issues induced by blasting operations, such as ground vibration, flyrock, air over-pressure, back-break, and dust (Afeni and Osasan 2009; Raina et al. 2011; Rezaei et al. 2011; Abbas and Asheghi 2018; Nguyen and Bui 2019). Of these issues, ground vibration, which is represented by peak particle velocity (PPV), was considered the most adverse effect induced by mine blasting (Ak et al. 2009; Nguyen et al. 2020). PPV is often used as the target variable of predictive models for predicting and evaluating ground vibration intensity because it is a dynamic response of buildings and it is closely related to ground vibration (Yan et al. 2020). In mine blasting, PPV can induce vibration of buildings/tunnels, instability, and even collapse of benches or slopes in open-pit/opencast mines, damage to structure of buildings, as well as threatening lives in neighboring communities (Tripathy and Gupta 2002; Singh and Singh 2005; Zgür Akkoyun and Taskıran 2015; Taheri et al. 2017; Tran et al. 2020).

To prevent and mitigate the damages caused by blast-induced ground vibration, many techniques have been proposed, such as improving the structure of buildings, using barriers to reduce ground vibration (Ekanayake et al. 2014), and predicting its vibration intensity (Nguyen et al. 2019c). So far, predicting ground vibration intensity (i.e., PPV) is considered as the state-of-the-art methodology because it allows adjustment of blasting parameters and mitigation of PPV before blasting. In this regard, soft computing (SC) and empirical models are considered as the most common approaches. Of those, SC models are well known as state-of-the-art techniques to predict and evaluate PPV with high accuracy and reliability (Murlidhar et al. 2020). Many scholars and researchers have, during the past decade, studied and proposed different artificial intelligence (AI) models as the SC models for predicting PPV with promising results (Table 1).

From Table 1, it can be seen that AI models have been proposed and widely applied in predicting PPV during the past decade. Although their performances are not similar because the datasets used and geological conditions are different per study, they are potential models for predicting PPV. Nevertheless, the differences have not been demonstrated in all areas, and the PPV induced by blasting operations in different locations/areas is not the same (Nguyen et al. 2019d; Kumar and Mishra 2020). Therefore, the main contribution of this study is to propose a novel hybrid AI model to predict PPV induced by blasting operations with high accuracy, aiming to reduce severe damages to surroundings.

The artificial neural network (ANN)-based cuckoo search optimization (CSO), named as CSO–ANN model, was proposed for this aim based on 118 blasting events that were collected at a quarry mine in Vietnam. Besides, stand-alone models, such as ANN, SVM, tree-based ensembles, and two empirical equations (i.e., USBM and Ambraseys), were also developed for comparison purposes. Finally, the developed models were tested and validated based on three blasting events in practical engineering.

ACADEMIC CONTRIBUTIONS

As reviewed above, many works have been published in terms of ground vibration-research and prediction. Various SC models have also been introduced and widely applied in this field. Nevertheless, their academic contributions and implications are different. This study contributes not only to blast-induced ground vibration-research and prediction but also to impact on further research, and specifically to the following.

The first academic contribution of this work to blast-induced ground vibration-research and prognosis is the generation of an integrative framework for predicting PPV based on the CSO algorithm and ANN. It addresses the process character of ground vibration prediction with various input variables, and how to predict PPV with the combination of the CSO algorithm and ANN. Herein, the potentials of the CSO algorithm are investigated to optimize an ANN model for predicting PPV.

The second contribution of this work is the application of deep learning in the development of

Table 1. Review of related work in predicting PPV using AI techniques in the past decade

References	AI technique	Input parameters	Performance
Khandelwal et al. (2010)	SVM	W, R	R^2 = 0.955; MAE = 0.226
Monjezi et al. (2010)	MLPNN	R, W, B/T, B_h, UCS, D_r	RMSE = 0.031
Khandelwal et al. (2011)	ANN	W, R	R^2 = 0.919; MAE = 0.352
Verma and Singh (2011)	GA	W, R	MAPE = 0.088
Fisne et al. (2011)	FL	W, R	RMSE = 5.31; VAF = 0.91
Hudaverdi (2012)	MA	B, S, H, T, U, D, PF	R^2 = 0.908; RMSE = 3.14; VAF = 82.29
Mohamadnejad et al. (2012)	SVM	W, R	r = 0.946; RMSE = 1.62
Monjezi et al. (2013)	ANN	W_{tt}, W, R	RMSE = 0.071; R^2 = 0.927; VAF = 92.68
Saadat et al. (2014)	ANN	W, R, S, H	RMSE = 8.796; R^2 = 0.957
Hasanipanah et al. (2015)	SVM	W, R	RMSE = 0.34; R^2 = 0.957; VAF = 94.24
Dindarloo (2015)	GEP	D, B_h, H_d, B, S, T, W, R, R_r	MAPE = 4.7; R^2 = 0.97
Hajihassani et al. (2015b)	PSO-ANN	H_d, W, B/S, T, U, PF, B_h, RQD, R	MSE = 0.038; R^2 = 0.89
Hajihassani et al. (2015a)	ICA-ANN	B/S, T, W, E, R	R^2 = 0.976; RMSE = 0.685
Armaghani et al. (2015)	ANFIS	D, H_d, W, B, S, T, PF, B_h	R^2 = 0.973; RMSE = 0.987; VAF = 97.345
Amiri et al. (2016)	ANN-KNN	W, R	R^2 = 0.88; VAF = 87.84; RMSE = 0.54
Monjezi et al. (2016)	GEP	W, R	R^2 = 0.918; RMSE = 2.321; VAF = 90.879
Ghoraba et al. (2016)	ANFIS	W, R	R^2 = 0.952; RMSE = 4.644
Hasanipanah et al. (2017a, b, c)	CART	W, R	R^2 = 0.950; RMSE = 0.170; NS = 0.948
Hasanipanah et al. (2017a)	GA	W, R	R^2 = 0.920; RMSE = 0.450; NS = 0.920; VAF = 93.230
Faradonbeh and Monjezi (2017)	GEP	B, S, T, D, H_d, W, B_h, PF, R	R^2 = 0.874; MAE = 5.164; RMSE = 6.732
Hasanipanah et al. (2017b)	PSO	W, R	R^2 = 0.938; NS = 0.940; VARE = 0.130; RMSE = 0.240
Taheri et al. (2017)	ABC-ANN	W, R	RMSE = 0.220; MAPE = 4.260; R^2 = 0.920
Shahnazar et al. (2017)	PSO-ANFIS	W, R	RMSE = 0.4835; R^2 = 0.984
Samareh et al. (2017)	PSO-GA	SD, B, S, DF, UCS, E_m, PF, I_s, W_{tt}, VoD, GSI	MSE = 60.260; RMSE = 7.760; VAF = 75.050; R^2 = 0.751
Abbas and Asheghi (2018)	GFNN	W, W_{tt}, R	MAPE = 1.310; RMSE = 0.157; VAF = 95.460; R^2 = 0.954
Armaghani et al. (2018)	ICA	W, R	RMSE = 0.370; R^2 = 0.940
Mokfi et al. (2018)	GMDH	B/S, H_d, T, PF, W, R	RMSE = 0.889; R^2 = 0.911
Sheykhi et al. (2018)	FCM-SVR	B, S, T, N_p, W, R	RMSE = 1.800; VAF = 85.250; R^2 = 0.853
Hasanipanah et al. (2018)	FS-ICA	W, R	RMSE = 0.220; VAF = 94.200; R^2 = 0.942
Zhang et al. (2019)	PSO-XGBoost	W, R, B, PF, S	RMSE = 0.583; MAE = 0.346; VAF = 96.083; R^2 = 0.968
Chen et al. (2019)	MFA-SVR	W, B/S, T, E, V_p, R	MAE = 0.556; RMSE = 0.614; R^2 = 0.984
Shang et al. (2019)	FFA-ANN	W, S, R, B, PF	RMSE = 0.464; VAF = 96.620; R^2 = 0.966; MAE = 0.356
Bui et al. (2019)	PSO-KNN	W, R	RMSE = 0.797; MAE = 0.385; R^2 = 0.977
Fang et al. (2019)	ICA-M5Rules	W, R, B, S	RMSE = 0.258; MAE = 0.175; R^2 = 0.995
Azimi et al. (2019)	GA-ANN	W, R, R_r, MR_r	R^2 = 0.988; MAPE = 60.011; RMSE = 3.047; VARE = 0.327; VAF = 99.828
Xue (2019)	FCM-ANFIS	W, R, SD	RMSE = 0.080; R^2 = 0.930; MAE = 0.062

Table 1. continued

References	AI technique	Input parameters	Performance
Yang et al. (2019)	ANFIS-GA	B, S, T, PF, W, R	R^2 = 0.979; RMSE = 0.240; VAF = 97.952; MAPE = 3.145; MAE = 0.199
Nguyen et al. (2019b)	HKM-CA	W, R, H, PF, B, S, T	R^2 = 0.995; MAE = 0.373; RMSE = 0.475
Hosseini et al. (2019)	MARS	$\underline{W}$, R	R^2 = 0.750; RMSE = 21.640; MAPE = 24.122
Nguyen et al. (2019a)	XGBoost	$\overline{W}$, H, B, S, T	R^2 = 0.952; RMSE = 1.742
Nguyen et al. (2019c)	BGAMs	W, R, H, PF, B, S	R^2 = 0.990; RMSE = 0.582; MAE = 0.430
Ding et al. (2019)	ICA-XGBoost	W, R, H, PF, B, S, T	R^2 = 0.988; RMSE = 0.736; MAE = 0.527
Nguyen et al. (2019e)	HKM-ANN	W, R, B, PF, S	R^2 = 0.983; VAF = 97.488; RMSE = 0.554
Nguyen et al. (2019d)	GA-SVR-RBF	W, R, B, S	R^2 = 0.991; RMSE = 0.267; VAF = 0.182
Yu et al. (2020a)	HHO-RF	W, W_{tt}, R, R_v, B, T_{dl}, f	PPV_{mean} = 10 mm/s; PPV $\leq$ 19.5 mm/s; the probability is 90%
Zhou et al. (2020)	FS-RF	S, B, R, W, H_d	Testing accuracy of 90.32%
Yu et al. (2020b)	RVM	W, W_{tt}, T_{dl}, B, R_v, R, f	RMSE = 0.045, R^2 = 0.971
Bayat et al. (2020)	FFA-ANN	B, S, R, W	RMSE = 4.380; VAF = 97.391; R^2 = 0.977; a20-index = 0.830

SVM (support vector machine); GEP (genetic expression programming); MLPNN (multilayer perceptron neural network), ANN (artificial neural network); MA (multivariate analysis); GA (genetic algorithm); FL (fuzzy logic); PSO (particle swarm optimization)-ANN; ANN-KNN (k nearest neighbors); ICA (imperialist competitive algorithm)-ANN; ANFIS (adaptive neuro-fuzzy inference system); ABC (artificial bee colony)-ANN; GFNN (generalized feed forward neural network); GMDH (group method of data handling); FCM (fuzzy C-means clustering)-SVR (support vector regression); FS (fuzzy system)-ICA; PSO-XGBoost (extreme gradient boosting machine); MFA (modified firefly algorithm)-SVR; FFA (firefly algorithm)-ANN; PSO-KNN; ICA-M5Rules; GA-ANN; FCM-ANFIS; ANFIS-GA; HKM-CA (hierarchical K-means clustering-cubist algorithm); MARS (multivariate adaptive regression splines); ICA-XGBoost; HKM-ANN; GA-SVR-RBF (radial basis function); HHO-RF (Harris Hawks optimization-random forest); RVM (relevance vector machine)
R (monitoring distance); W (explosive charge per delay); B/S (ratio of burden and spacing); B_h (number of boreholes); UCS (uniaxial compressive strength of rock mass); D_r (delay per rows); S (spacing); H (bench height); U (sub-drilling); D (borehole diameter); PF (powder factor); W_{tt} (total explosive charged); H_d (hole depth); R_r (radial distance); T (stemming); RQD (rock-quality designation); E (Young modulus); E_s (deformation modulus); DF (discontinuity frequency); I_s (impedance); VoD (velocity of detonation); GSI (geological strength index); N_p (number of boreholes per delay); V_p (p wave velocity); MR_r (modified radial distance); SD (scaled distance); R_v (vertical distance); T_{dl} (delay time of detonator); f (Protodyakonov's impact strength coefficient)
R^2 (determination of coefficient); r (correlation coefficient); VARE (variance absolute relative error); MAE (mean absolute error); NS (Nash and Sutcliffe); MAPE (mean absolute percentage error); VAF (variance accounted for); MSE (mean-squared error)

the ANN model for improving the accuracy of the ANN model before optimizing this model by the CSO algorithm. Typically, scholars often use deep learning techniques or optimization algorithms for the aim of enhancing the model's performance. However, in this study, we used both approaches to improve the performance of the ANN model in predicting PPV. Thus, deep learning was used as the first step, and the CSO algorithm (optimization algorithm) was applied as the next step to improve the model's accuracy.

The third contribution of this work is the investigation of the effect of the total explosive charge per blast and the maximum amount of explosive charge per borehole on blast-induced ground vibration. The results of the current research will contribute to implications for further study in the future based on the role of these parameters and the blasting method applied.

STUDY SITE AND DATASET USED

This study was undertaken in the Thuong Tan 3 quarry mine in Binh Duong province (Vietnam) (Fig. 1). The geological structure of the mine is relatively simple. The base rocks are limestone and calcareous siltstone of the Draylinh Formation; these rocks are located intertwined. These rocks are not exposed on the surface but are covered with clay and mixed clay deposits sandwiched with sand-phase lenses of the Quaternary complex with average thickness of 7–8 m. In this mine, the rocks are mainly quarried are tuff rhyolite with Protodyakonov's impact strength coefficient of 12. The

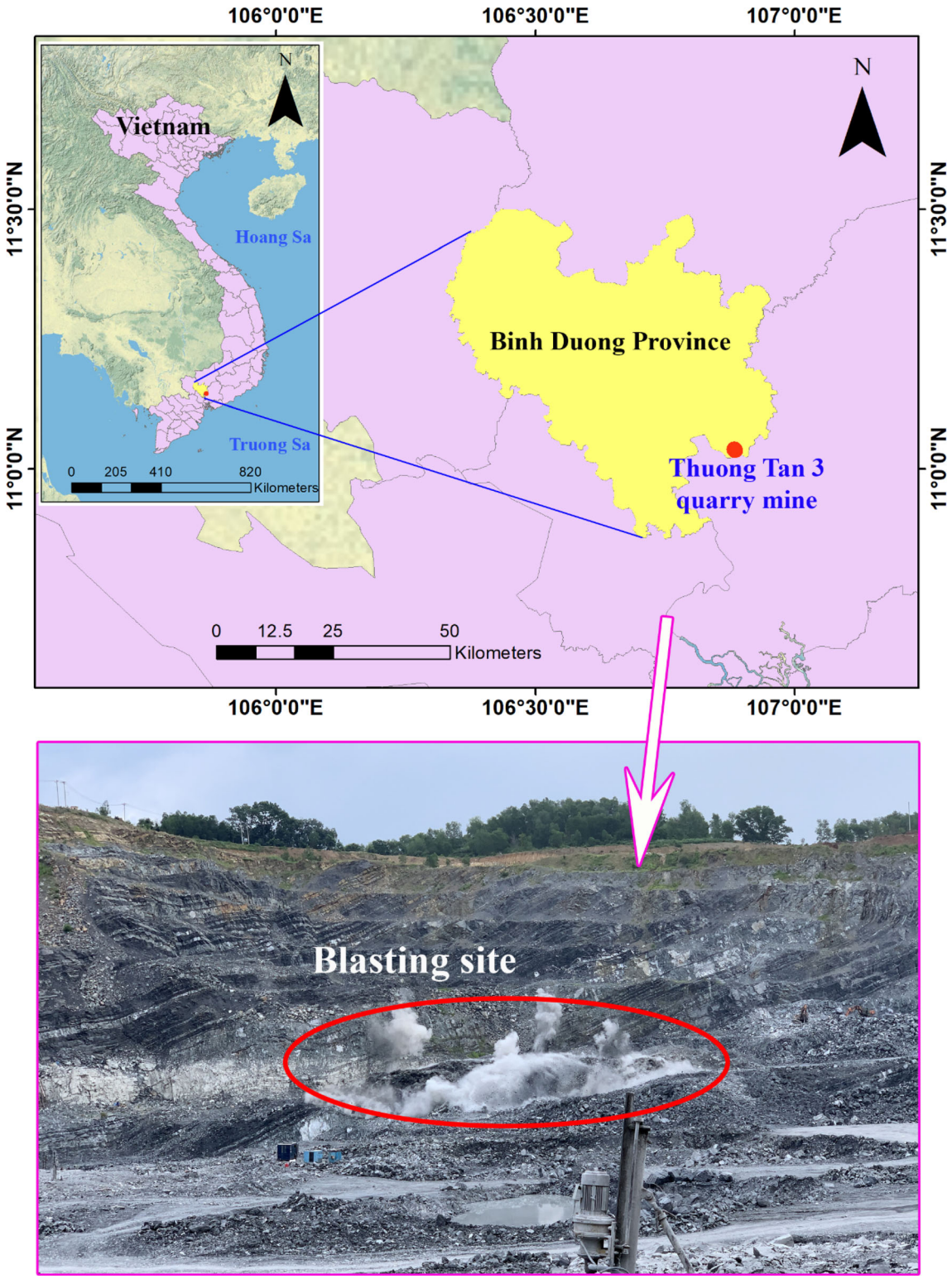

Figure 1. Location and a view of the Thuong Tan 3 quarry mine (Vietnam).

compressive strength of this rock is in the range of 741–1332 kg/cm^2 for the dry state and 693–1261 kg/cm^2 for the saturated state. Thus, blasting is taken as an effective method for breaking and moving rock mass in this mine.

In order to fragment rock mass, blasts are carried out in benches with bench high in the range of 7.9–11.5 m. Before blasting, boreholes are drilled with a diameter of 105 mm and the hole depth in the range of 9–12.5 m. For each blast site, the number of boreholes is in the range of 45–66 boreholes. The primary explosives used are NT ϕ80 and ANFO, and the delay time of the millisecond-delay blasting method was applied with the use of digital electronic detonators. The maximum explosive charge per blast is 3000 kg and 57 kg for the mass explosive per hole.

For data collection, two groups of the dataset were divided, including the blasting parameters (i.e., input variables) and PPV (i.e., output variable). In this study, the total explosive charge per blast (W_{tt}), the amount of explosive per hole (W_{bh}), PPV measuring distance (R), spacing (S), burden (B), and powder factor (PF) were used as the input variables.

As mentioned by many previous researchers, monitoring distance, spacing, burden, and powder factor are the parameters that are often used to predict PPV. However, previous studies only considered the maximum explosive charge per delay or the total explosive per blast, but ignored the maximum amount of explosive charge per borehole. Therefore, in this study, the effect of the maximum amount of explosive charge per borehole was considered, and it was also used as one of the input variables to predict PPV.

A global positioning sensor (GPS) receiver was used to measure the distance between the positions of blast sites and seismograph points. The other input variables were extracted from the blast pattern by blasting engineers. To estimate PPV, the Micromate seismograph (Instantel) was used (Fig. 2). Finally, 118 blasting events were recorded at this mine, and the dataset used is summarized in Table 2.

METHODOLOGY

As introduced above, the primary aim of this study was to investigate and propose a novel hybrid CSO-ANN model for PPV prediction in opencast/open-pit mines, and it was undertaken at the Thuong Tan 3 quarry mine (Vietnam). Subsequently, an ANN model (without optimization), SVM, tree-based ensembles, and two empirical equations were also applied/developed for comprehensive comparison and assessment to prove the enhanced performance of the proposed CSO–ANN model. Because the respective principles of the SVM and tree-based ensembles have been introduced and discussed in many papers (e.g., Hearst et al. 1998; Borisov et al. 2006; Ma and Guo 2014; Ayaz et al. 2015; Abolfathi et al. 2016; Kaveh et al. 2016; Gholami and Fakhari 2017; Besler et al. 2019; Efthymiou et al. 2019; Nguyen et al. 2019f; Joshi 2020; Tran 2020), they are not presented in this section. Only the respective principles of CSO, ANN, the framework of the CSO-ANN model, empirical equations, and evaluation criteria are introduced in this section.

Artificial Neural Network

ANN is a state-of-the-art SC technique in computer science or mathematics during the past decades. It is inspired by the functional aspects or structure of the human brain or biological neural networks. Accordingly, a group of neurons/nodes is interconnected in an ANN, and it manages the information by the approach of connectionist to computing the weights of the neurons/nodes (Daniel 2013; Nguyen and Tong 2020). The artificial neurons or nodes of an ANN model are often divided into three types of layers, including input layer, hidden layer(s), and output layer. Each layer and each neuron are connected through weights (maybe negative or positive), which are not similar for different training algorithms.

To train ANN models, many algorithms can be applied, such as feed-forward, back-propagation, Levenberg–Marquardt, quick propagation, to name a few (Can et al. 2019). During training of ANN models, transfer functions (active functions) are often used to avoid over-fitting and to improve the accuracy of an ANN model (Vu et al. 2020). Typical transfer functions are linear/nonlinear, sigmoid, adam, relu, to name a few (Zou et al. 2008; Prasad et al. 2012; Feng et al. 2015; Ye et al. 2020).

A review of the literature shows that ANN is the most common model that has been developed and applied in real-life problems, especially in the mining industry (Nerguizian et al. 2006; Huang et al. 2018). In terms of PPV prediction, ANN is one of the most popular models as well, and it was often combined with metaheuristic algorithms (optimiza-

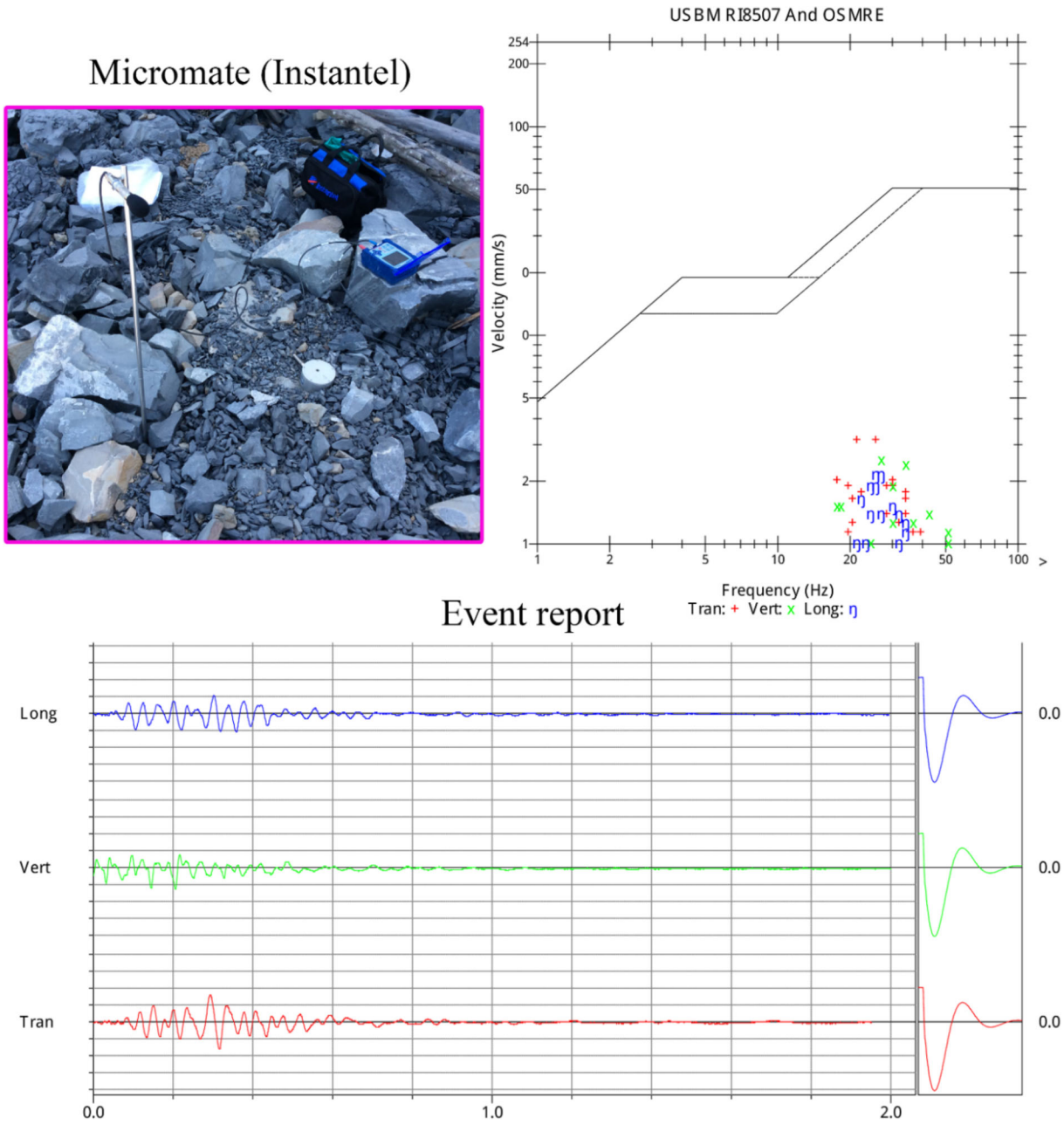

Figure 2. Seismograph and an event report of ground vibration in the study site.

tion algorithms) to optimize the accuracy and errors of the model (Table 1). In this study, ANN was used as the main technique to predict PPV and it then was optimized by the CSO algorithm to reduce the error and thus improve the accuracy of the ANN model. An ANN structure for PPV prediction is shown in Figure 3.

Cuckoo Search Optimization

Cuckoo search optimization (CSO) was introduced by Yang and Deb (2009) for optimization problems, and it is well known as a metaheuristic algorithm. It was introduced and designed based on the behavior of cuckoo bird in terms of obligate

Table 2. Summary of the input and output variables used for predicting PPV

Category	W_{tt}	W_{bh}	R	S	B	PF	PPV
Min	1936	32	198.8	3.1	3.1	0.4	0.458
1st Quartile	2796	40	273.4	3.4	3.2	0.44	1.659
Median	2971	46	351.7	3.4	3.2	0.45	2.796
Mean	2782	45.79	364.7	3.417	3.227	0.4404	3.246
3rd Quartile	3000	53.5	439.7	3.5	3.3	0.45	4.521
Max	3000	57	750	3.7	3.4	0.45	11.17

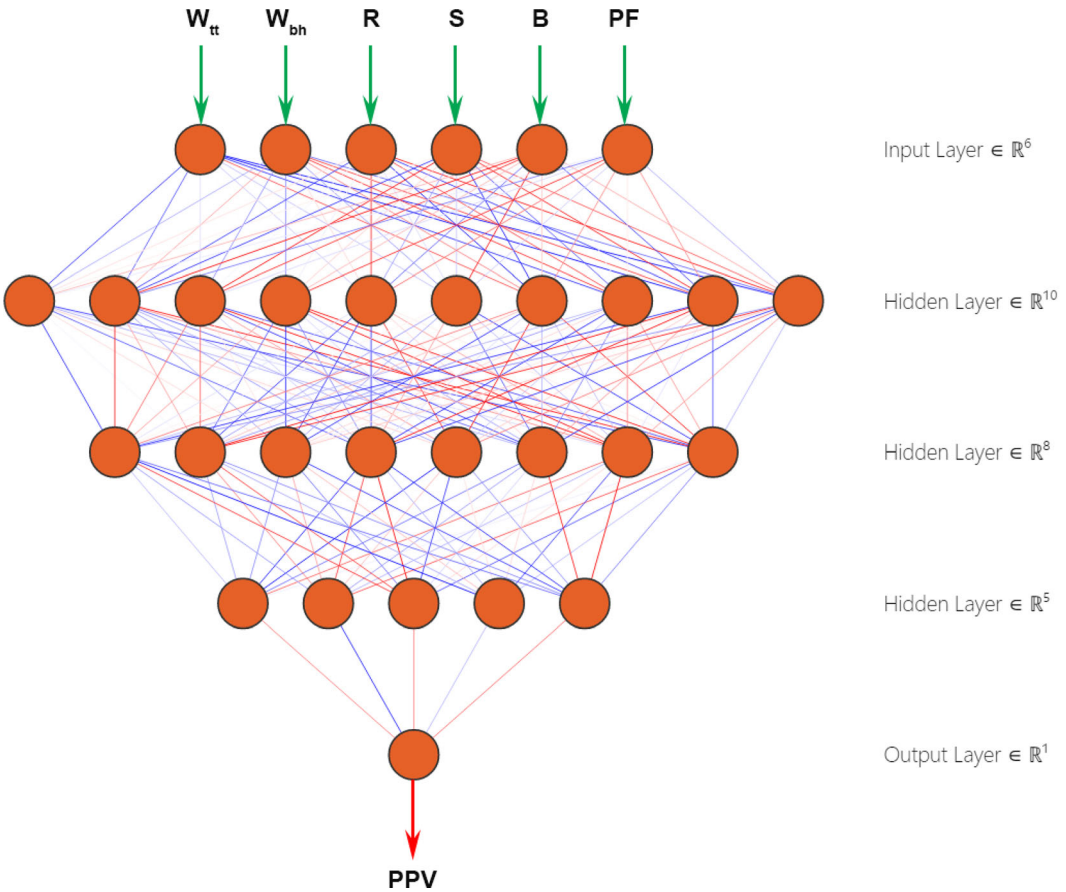

Figure 3. An ANN structure for PPV prediction with three hidden layers.

brood parasitic and the Lévy flight algorithm. The CSO algorithm performs three tasks and rules (Fig. 4).

Based on the rules (Fig. 4), the CSO algorithm can maintain a balance (b_a) between global random walk (G_{rw}) and local random walk (L_{rw}). Therefore, it is considered as a robust global optimization solution. It is worth noting that a switching parameter p_a can control the b_a. The (L_{rw}) and (G_{rw}) can be calculated, respectively, by the following equations:

$$x_i^{t+1} = x_i^t + \beta s \Theta F \varsigma (p_a - \delta) \Theta \left(x_j^t - x_k^t \right) \quad (1)$$

$$x_i^{t+1} = x_i^t + \beta L(\varsigma, \lambda) \quad (2)$$

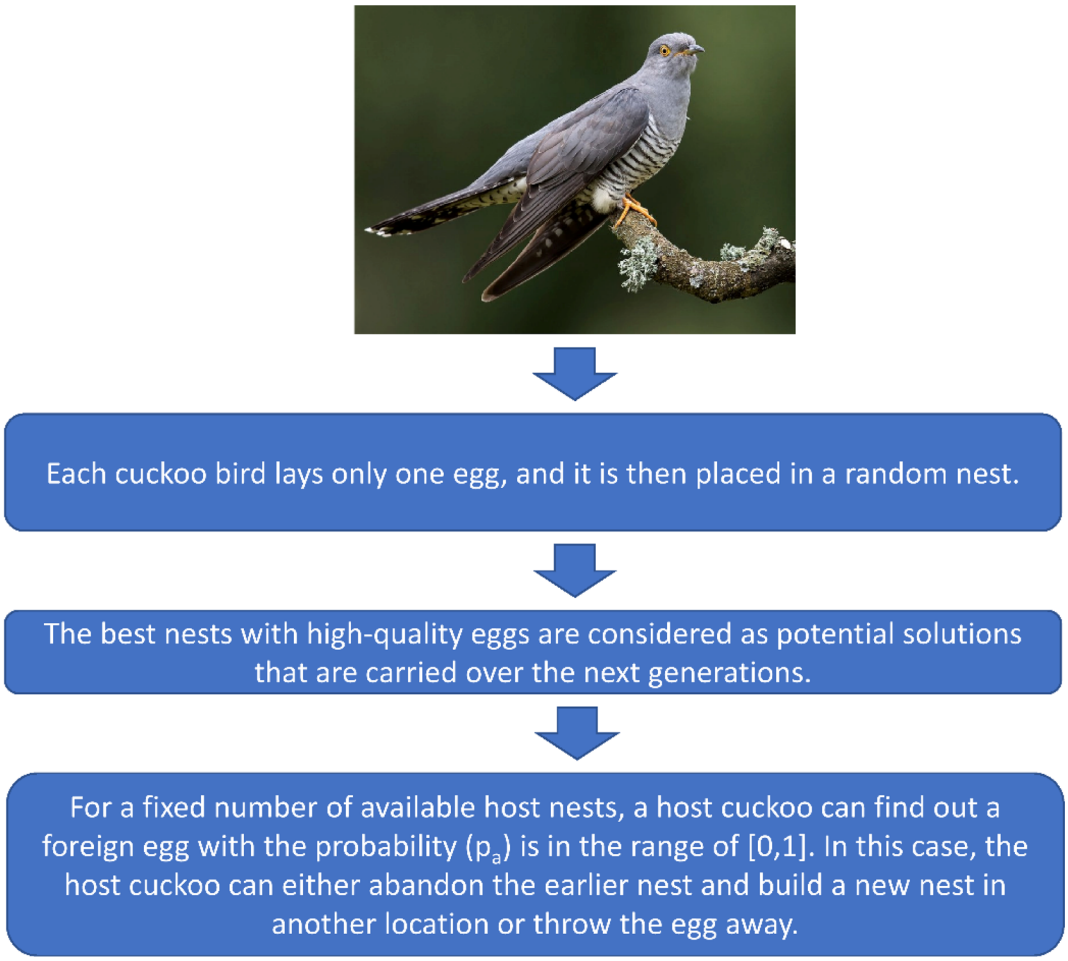

Figure 4. Rules of the CSO algorithm.

where β is the scaling factor with positive step sizes and $\beta>0$; ς is the step size; F denotes the function of heavy-side; Θ represents entry-wise multiplications; δ is the random number of uniform distribution; x_i^t, x_j^t, x_k^t stand the current positions; $L(\varsigma, \lambda)$ is the Lévy distribution. The algorithm development process of the CSO algorithm is described in the pseudo-code (Fig. 5). Further details of the CSO algorithm can be found in the literature (Yang and Deb 2009, 2014; Gandomi et al. 2013; Wang et al. 2016; Mareli and Twala 2018).

ANN-based Cuckoo Search Optimization

As mentioned above, ANN is one of the most common methods used not only for predicting PPV but also for solving many real-life problems. However, the crucial issues of an ANN model are its structure, weights and biases; addressing these is challenging for development of an optimal ANN model. Therefore, many researchers applied optimization algorithms to address those issues with promising results (e.g., Leardi 2003; Mirjalili et al. 2012; Jafarian et al. 2013; Kaydani and Mohebbi 2013; Zăvoianu et al. 2013; Aljarah et al. 2018).

Regarding prediction of PPV in open-pit mines, many optimization algorithms have been applied to enhance the ANN model (Table 1). Most of them are based on the optimization mechanism of weights and biases to reduce the error of the predictive model. Nevertheless, the CSO algorithm has not been considered for the optimization of ANN in predicting PPV. Hence, this section proposes the

Algorithm 1: Cuckoo search optimization

Set the initial value of the host nest size n, probability $p_a \in [0, 1]$ and maximum number of iterations Max_{itr}.
Set $t := 0$. {Counter initialization}
for $(i = 1 : i \leq n)$ **do**
    Generate initial population of n host $x_i^{(t)}$. {n is the population size}
    Evaluate the fitness function $f(x_i^{(t)})$.
end for
repeat
    Randomly generate a new solution (Cuckoo) $x_i^{(t+1)}$ by Lévy flight.
    Evaluate the fitness function of a solution $x_i^{(t+1)}$ $f(x_i^{(t+1)})$
    Randomly choose a nest x_j among n solutions.
    if $(f(x_i^{(t+1)}) > f(x_j^{(t)}))$ **then**
        Replace the solution x_j with the solution $x_i^{(t+1)}$
    end if
    Abandon a fraction p_a of worse nests.
    Build new nests at new locations using Lévy flight a fraction p_a of worse nests
    Keep the best solutions (nests with quality solutions)
    Rank the solutions and find the current best solution
    Set $t = t + 1$.
until $(t \geq Max_{itr})$. {Termination criteria are satisfied}
Produce the best solution.

Figure 5. Pseudo-code of the CSO algorithm.

framework of the CSO–ANN model for PPV prediction.

Generally, preparation and normalization of a dataset are often adopted before developing any AI models. Here, the dataset was pre-processed as a mandatory procedure to avoid over-fitting of the models. Next, an ANN model with initial weights and biases is established for PPV prediction. Subsequently, the CSO algorithm performs a global search to find out the optimal parameters of the established ANN model. The searching process is conducted continuously to get the optimal weights and biases. Then, the error is calculated, and the criterion stopping is checked for determining the optimal CSO–ANN model through the objective function (i.e., RMSE). The flowchart of the proposed CSO–ANN network for PPV prediction is shown in Figure 6.

Empirical Equations

Empirical equations are considered rapid determination methods of PPV because of their inherently simple calculations. Accordingly, they often use only total explosive charge per blast (or maximum explosive charge per delay) and monitoring distance as the primary input variables for estimating PPV. The equations of the United States Bureau of Mines (USBM) (Duvall and Fogelson 1962) and Ambraseys (1968) have been used as the most famous empirical equations for estimating PPV. Therefore, they were used in this study for comparison purposes, and they are defined as follows:

$$\text{(i) USBM equation : PPV} = \lambda\left(\frac{R}{\sqrt{W}}\right)^{-\alpha} \quad (3)$$

$$\text{(ii) Ambraseys equation : PPV} = \lambda\left(\frac{R}{\sqrt[3]{W}}\right)^{-\alpha} \quad (4)$$

where λ and α are the site coefficients, and they are calculated based on multivariate regression analysis of the dataset used.

Evaluation Criteria

To assess the efficiency as well as the stability of the developed PPV predictive models, as well as to

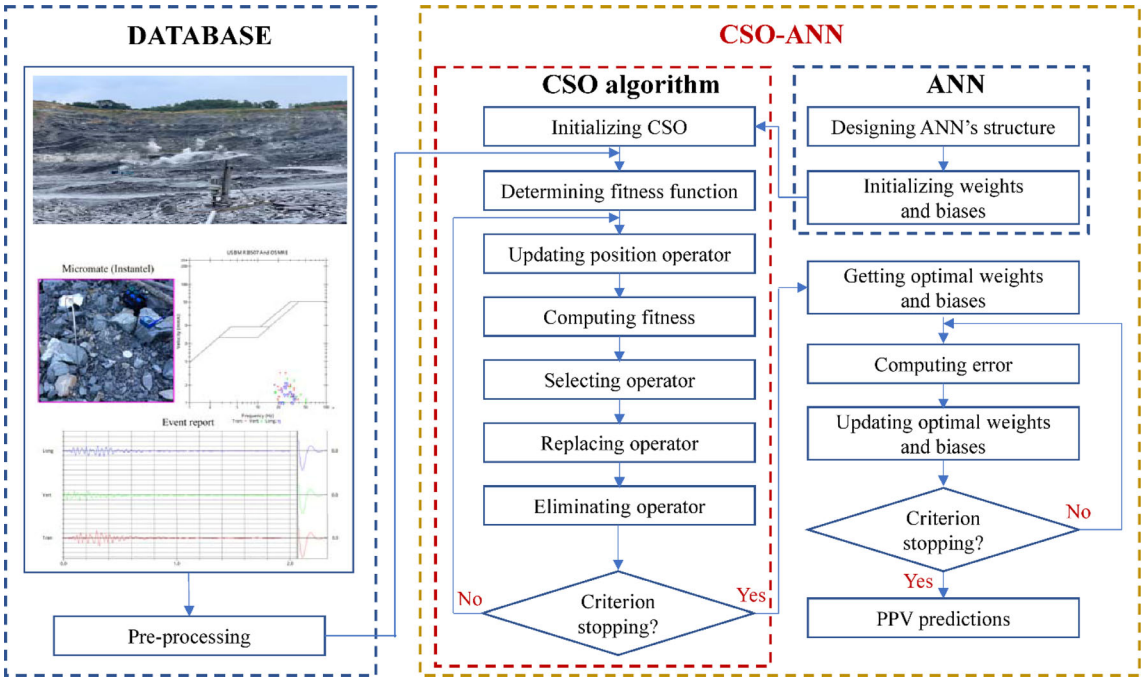

Figure 6. Flowchart of the proposed CSO–ANN hybrid model for predicting PPV.

have a comprehensive comparison of their performance, MAE, RMSE, R^2, VAF, and a20-index were used as performance metrics in this study. They are computed as follows.

$$\mathrm{MAE} = \frac{1}{n_{\mathrm{blast}}} \sum_{i=1}^{n_{\mathrm{blast}}} |y_{i\_\mathrm{PPV}} - \hat{y}_{i\_\mathrm{PPV}}| \tag{5}$$

$$\mathrm{RMSE} = \sqrt{\frac{1}{n_{\mathrm{blast}}} \sum_{i=1}^{n_{\mathrm{blast}}} (y_{i\_\mathrm{PPV}} - \hat{y}_{i\_\mathrm{PPV}})^2} \tag{6}$$

$$R^2 = 1 - \frac{\sum_{i=1}^{n_{\mathrm{blast}}} (y_{i\_\mathrm{PPV}} - \hat{y}_{i\_\mathrm{PPV}})^2}{\sum_{i=1}^{n_{\mathrm{blast}}} (y_{i\_\mathrm{PPV}} - \overline{y}_{i\_\mathrm{PPV}})^2} \tag{7}$$

$$\mathrm{VAF} = \left(1 - \frac{\mathrm{var}\left(y_{i\_\mathrm{PPV}} - \hat{y}_{i\_\mathrm{PPV}}\right)}{\mathrm{var}(y_{i\_\mathrm{PPV}})}\right) \times 100 \tag{8}$$

$$\text{a20 - index} = \frac{m20}{n_{\mathrm{blast}}} \tag{9}$$

where n_{blast} is number of blasting events; y_{i_PPV}, $\hat{y}_{i\_\mathrm{PPV}}$, and $\overline{y}_{i\_\mathrm{PPV}}$ are the ith PPV measured, predicted, and mean of measured values, respectively; m20 is number of samples in the range of 80% confidence level (between 0.80 and 1.20).

CONFIGURATION AND TRAINING OF MODELS

ANN Model

In order to train the ANN model for PPV prediction, a deep learning technique with a different number of hidden layers and neurons was applied to determine the optimal structure of the ANN model (Fig. 7). As a data pre-processing step, the MinMax scale [0,1] was used to avoid over-fitting of the ANN model. Then, the ANN model with structure of 6–18–16–6–1 (3 hidden layers) was determined and used for predicting PPV in this study (Fig. 8).

CSO–ANN Model

To build the CSO–ANN model, the CSO algorithm was coupled with the ANN model based on the principle that was proposed in Figure 6.

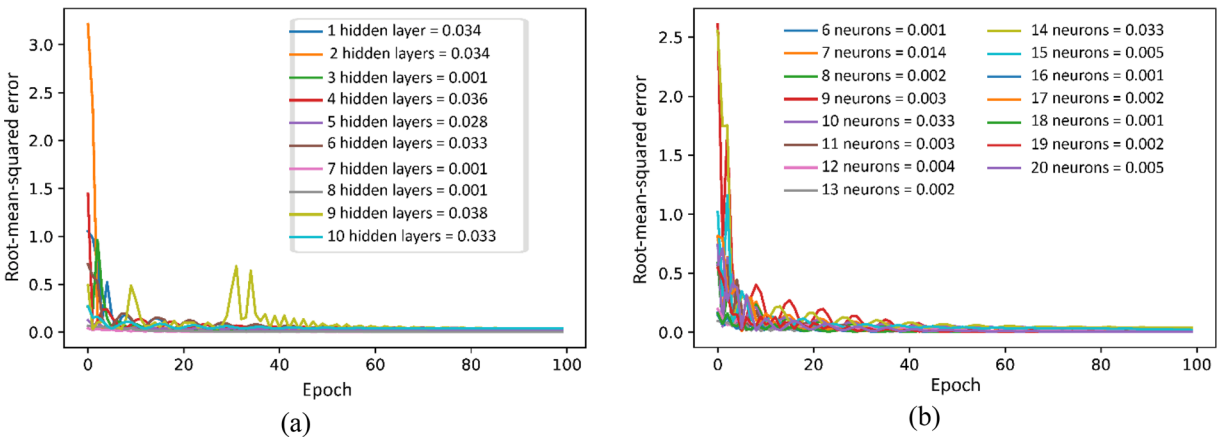

Figure 7. Deep learning for selection of optimal ANN structure: **a** RMSE of different hidden layers; **b** RMSE of different hidden neurons.

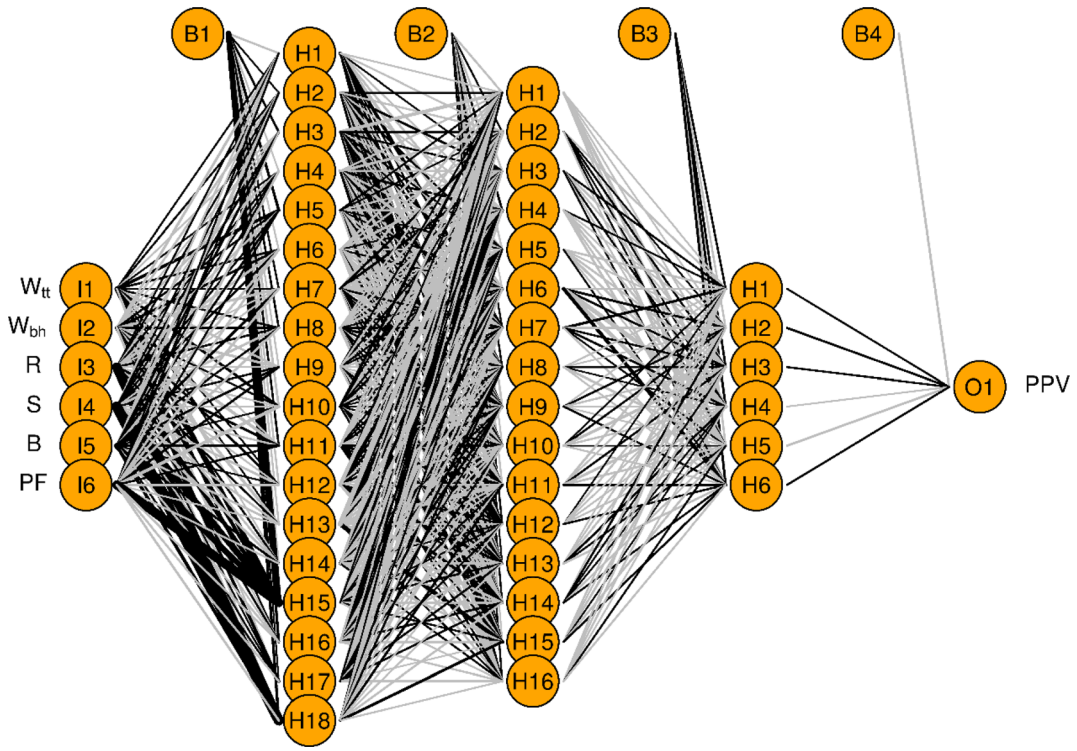

Figure 8. Optimal structure of the ANN model for PPV prediction.

Accordingly, the weights and biases of the initial ANN model (i.e., 6–18–16–6–1) were optimized by the CSO algorithm. RMSE was used as the objective function during the training and optimizing the ANN model. Before training the ANN model, the parameters of the CSO algorithm were set up, and they were selected as follows: $p_a = 0.25$; step size $(s) = 0.01$; Lévy flight $(L) = 1.6$. In addition, the number of cuckoo birds that has a significant effect on the performance of the optimization process was

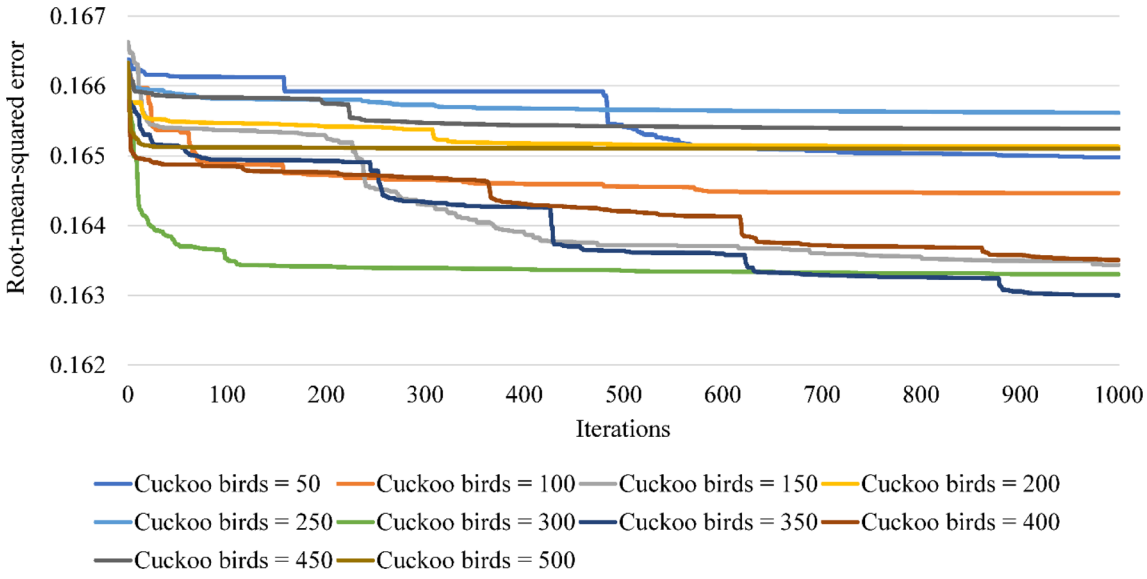

Figure 9. RMSE of the proposed CSO-ANN model in PPV prediction (training phase).

defined. Therefore, the global search of cuckoo birds was conducted with different numbers of cuckoo birds, i.e., 50, 100, 150, 200, 250, 300, 350, 400, 450, 500. To satisfy stopping conditions, the global search of the CSO–ANN model was performed for 1000 iterations. The performance of the CSO–ANN model in training and predicting PPV is shown in Figure 9. Eventually, the optimal CSO–ANN model (with RMSE = 0.163) was defined with 350 cuckoo birds and iterations of 979.

SVM Model

In order to build the SVM model for PPV prediction, the radial basis kernel function was applied with C(cost) and σ used as the principal coefficients to control the accuracy of the SVM model. One hundred SVM models with different ranges of C and σ were checked to find the best SVM model for predicting PPV in this study. A tenfold cross-validation (CV) technique and the Box-Cox transformation were applied to normalize the dataset used to avoid over-fitting of the models. Ultimately, the best SVM model was defined with $C = 23.460$ and $\sigma = 0.019$. More details of 100 SVM models are presented in Table 3. Notably, the training dataset used for the configuration of the SVM model is the same as those used for the previous models.

Tree-Based Ensembles Model

For the tree-based ensembles modeling, the maximum interaction depth and the prediction mode (e.g., mean and outbag) were used to adjust the accuracy of the tree-based ensembles model. A similar techniques as above, namely tenfold CV, Box-Cox transformation, and grid search, were applied for the development of the tree-based ensembles model. The maximum interaction depth was set in the range of 1–20 with trial-and-error procedure of the prediction mode (i.e., mean or outbag) (Fig. 10). Finally, the best tree-based ensembles model was developed with the maximum interaction depth of 6 using the ‘‘mean’’ prediction mode.

Empirical Models

To configure the empirical models, Eqs. (3) and (4) were applied to the training dataset to find the site coefficients. It is worth noting that the empirical models were developed based on the same training dataset as those developed for the AI models (i.e., SVM, ANN, CSO-ANN, and tree-based ensembles). Multivariate regression analysis was applied to calculate the site coefficients based on Eqs. (3) and (4). Eventually, two official empirical equations were proposed for estimating PPV in this study, thus:

Table 3. Performance measures of different SVM models for PPV prediction. The best predictive model is highlighted in bold

No	σ	C	RMSE	R^2	MAE	No	σ	C	RMSE	R^2	MAE
1	0.008	383.617	0.368	0.977	0.228	51	0.141	0.219	0.659	0.938	0.424
2	0.009	2.831	0.541	0.949	0.351	52	0.177	0.346	0.586	0.948	0.362
3	0.010	0.045	1.840	0.855	1.479	53	0.180	0.131	0.886	0.903	0.590
4	0.010	0.040	1.856	0.855	1.492	54	0.188	562.255	0.560	0.921	0.367
5	0.011	0.243	1.051	0.883	0.770	55	0.196	0.070	1.237	0.858	0.884
6	0.011	208.810	0.367	0.977	0.227	56	0.216	71.964	0.493	0.953	0.331
7	0.012	3.901	0.473	0.960	0.303	57	0.222	3.196	0.482	0.961	0.299
8	0.013	13.728	0.381	0.973	0.240	58	0.312	5.045	0.502	0.956	0.324
9	0.015	206.931	0.375	0.977	0.232	59	0.478	501.630	0.807	0.832	0.482
10	0.016	0.274	0.868	0.904	0.610	60	0.551	0.392	0.766	0.916	0.491
11	0.016	0.580	0.666	0.931	0.436	61	0.650	13.683	0.619	0.928	0.417
12	0.016	814.147	0.438	0.968	0.273	62	0.662	0.931	0.676	0.923	0.432
13	**0.019**	**23.460**	**0.366**	**0.976**	**0.226**	63	0.669	0.202	1.046	0.877	0.724
14	0.019	0.069	1.520	0.860	1.186	64	0.678	0.077	1.548	0.787	1.168
15	0.019	0.491	0.675	0.930	0.444	65	0.678	997.127	1.034	0.723	0.590
16	0.019	43.173	0.368	0.977	0.229	66	0.895	0.660	0.780	0.906	0.512
17	0.020	78.083	0.370	0.977	0.229	67	0.916	2.026	0.714	0.913	0.474
18	0.024	5.517	0.382	0.974	0.244	68	0.921	475.392	0.934	0.768	0.567
19	0.026	634.875	0.460	0.966	0.299	69	0.937	0.034	1.855	0.625	1.444
20	0.026	0.168	0.914	0.896	0.642	70	0.938	1.215	0.747	0.908	0.484
21	0.028	31.972	0.367	0.977	0.231	71	0.947	48.029	0.713	0.891	0.471
22	0.028	1.739	0.464	0.962	0.295	72	1.078	26.915	0.732	0.896	0.495
23	0.028	0.060	1.457	0.862	1.122	73	1.131	2.294	0.765	0.900	0.514
24	0.028	8.164	0.373	0.975	0.234	74	1.170	138.105	0.854	0.831	0.552
25	0.038	2.183	0.401	0.971	0.256	75	1.310	579.951	0.939	0.780	0.597
26	0.038	0.048	1.492	0.863	1.149	76	1.311	136.065	0.881	0.820	0.576
27	0.044	18.444	0.381	0.976	0.239	77	1.321	13.352	0.790	0.884	0.542
28	0.046	0.738	0.513	0.956	0.326	78	1.328	35.163	0.790	0.872	0.535
29	0.049	3.910	0.387	0.973	0.244	79	1.366	438.786	0.937	0.782	0.603
30	0.050	0.111	0.952	0.891	0.661	80	1.415	2.273	0.830	0.881	0.566
31	0.054	62.569	0.421	0.972	0.270	81	1.443	1.321	0.868	0.876	0.579
32	0.055	27.938	0.402	0.975	0.253	82	1.451	0.184	1.406	0.768	1.023
33	0.055	0.031	1.623	0.863	1.266	83	1.601	117.870	0.915	0.811	0.616
34	0.057	0.829	0.467	0.962	0.298	84	1.754	57.054	0.903	0.830	0.620
35	0.060	41.372	0.419	0.973	0.267	85	2.103	0.223	1.451	0.734	1.064
36	0.065	40.624	0.423	0.972	0.271	86	2.131	0.146	1.621	0.678	1.226
37	0.065	8.006	0.393	0.974	0.248	87	2.170	9.018	0.929	0.833	0.654
38	0.066	19.752	0.406	0.974	0.257	88	2.224	0.154	1.615	0.679	1.220
39	0.071	4.267	0.399	0.972	0.249	89	2.245	1.673	0.985	0.831	0.680
40	0.072	38.836	0.427	0.972	0.275	90	2.297	0.041	1.914	0.442	1.499
41	0.073	6.530	0.400	0.973	0.253	91	2.417	436.374	0.975	0.795	0.684
42	0.077	11.450	0.406	0.974	0.259	92	2.578	30.107	0.966	0.807	0.684
43	0.078	0.109	0.931	0.893	0.638	93	2.691	0.157	1.656	0.645	1.257
44	0.078	0.158	0.782	0.911	0.519	94	2.702	260.413	0.988	0.793	0.699
45	0.078	3.940	0.406	0.971	0.254	95	2.789	7.654	0.996	0.808	0.710
46	0.084	6.143	0.408	0.972	0.259	96	2.835	11.138	0.993	0.806	0.709
47	0.118	14.825	0.440	0.969	0.282	97	2.845	2.960	1.018	0.806	0.721
48	0.120	268.770	0.531	0.947	0.350	98	2.921	1.515	1.068	0.800	0.746
49	0.128	25.593	0.447	0.967	0.290	99	2.978	0.084	1.817	0.492	1.407
50	0.129	0.066	1.203	0.865	0.855	100	3.158	0.090	1.812	0.493	1.401

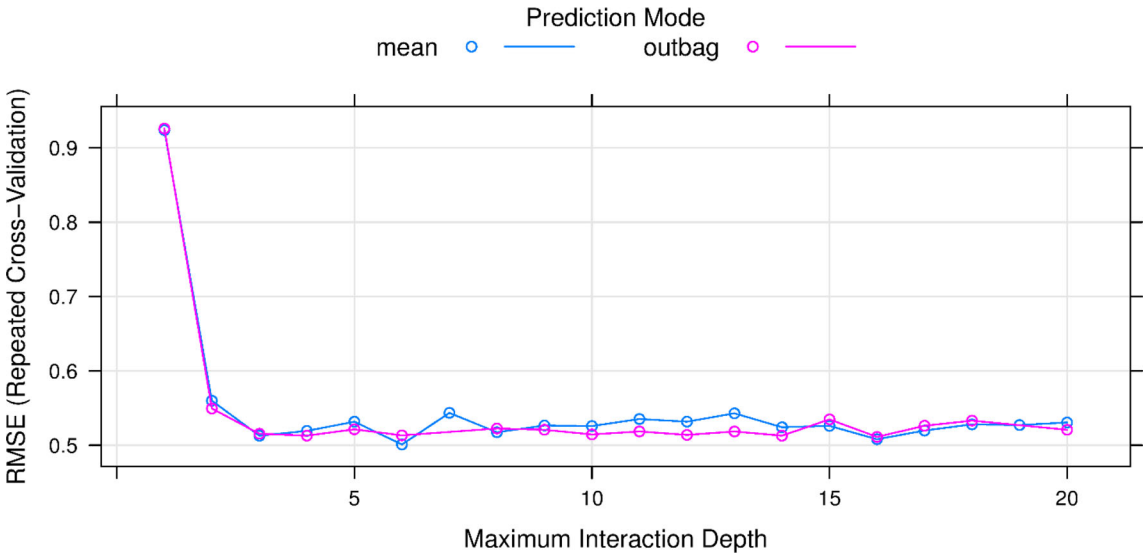

Figure 10. Performance of the tree-based ensembles model on the training phase.

Table 4. Overall performance and the error of the models developed

Model	Training phase					Testing phase				
	MAE	RMSE	R2	VAF	a20-index	MAE	RMSE	R2	VAF	a20-index
ANN	0.153	0.276	0.982	98.226	0.948	0.172	0.257	0.987	98.542	0.955
CSO-ANN	0.108	0.163	0.994	99.383	0.979	0.178	0.246	0.990	98.668	1.000
SVM	0.226	0.366	0.976	97.625	0.914	0.256	0.503	0.960	94.482	0.909
Tree-based ensembles	0.306	0.501	0.953	95.058	0.893	0.308	0.652	0.932	90.869	0.864
USBM empirical	1.261	1.701	0.361	36.033	0.198	1.389	1.902	0.229	21.023	0.227
Ambraseys empirical	1.258	1.705	0.360	35.949	0.198	1.395	1.905	0.227	20.942	0.227

$$\text{(iii) USBM equation : PPV} = 41.273\left(\frac{R}{\sqrt{W}}\right)^{-1.461} \tag{8}$$

$$\text{(iv) Ambraseys equation : PPV} = 332.088\left(\frac{R}{\sqrt[3]{W}}\right)^{-1.510} \tag{9}$$

RESULTS AND DISCUSSION

Once the AI and empirical models were well configured, performance measures (i.e., MAE, RMSE, R^2, VAF, and a20-index) are computed for the observations in the testing dataset to verify the training performance, as well as to evaluate the overall performance of the models. Further, the proposed hybrid CSO–ANN model was compared with the other models, i.e., ANN, SVM, tree-based ensembles, USBM and Ambraseys empirical equations. The comparative prediction results of the developed models are summarized in Table 4.

From Table 4, we can see that the empirical models are a failure in this study because of high errors (i.e., MAE and RMSE), and their R^2 values also indicate that they are not suitable for the database used in this study; the VAF and a20-index also revealed the weakness of the empirical models. In contrast, the four AI models modeled PPV very well, and all of them overcame the over-fitting issue. This finding indicates that the PPV should not be

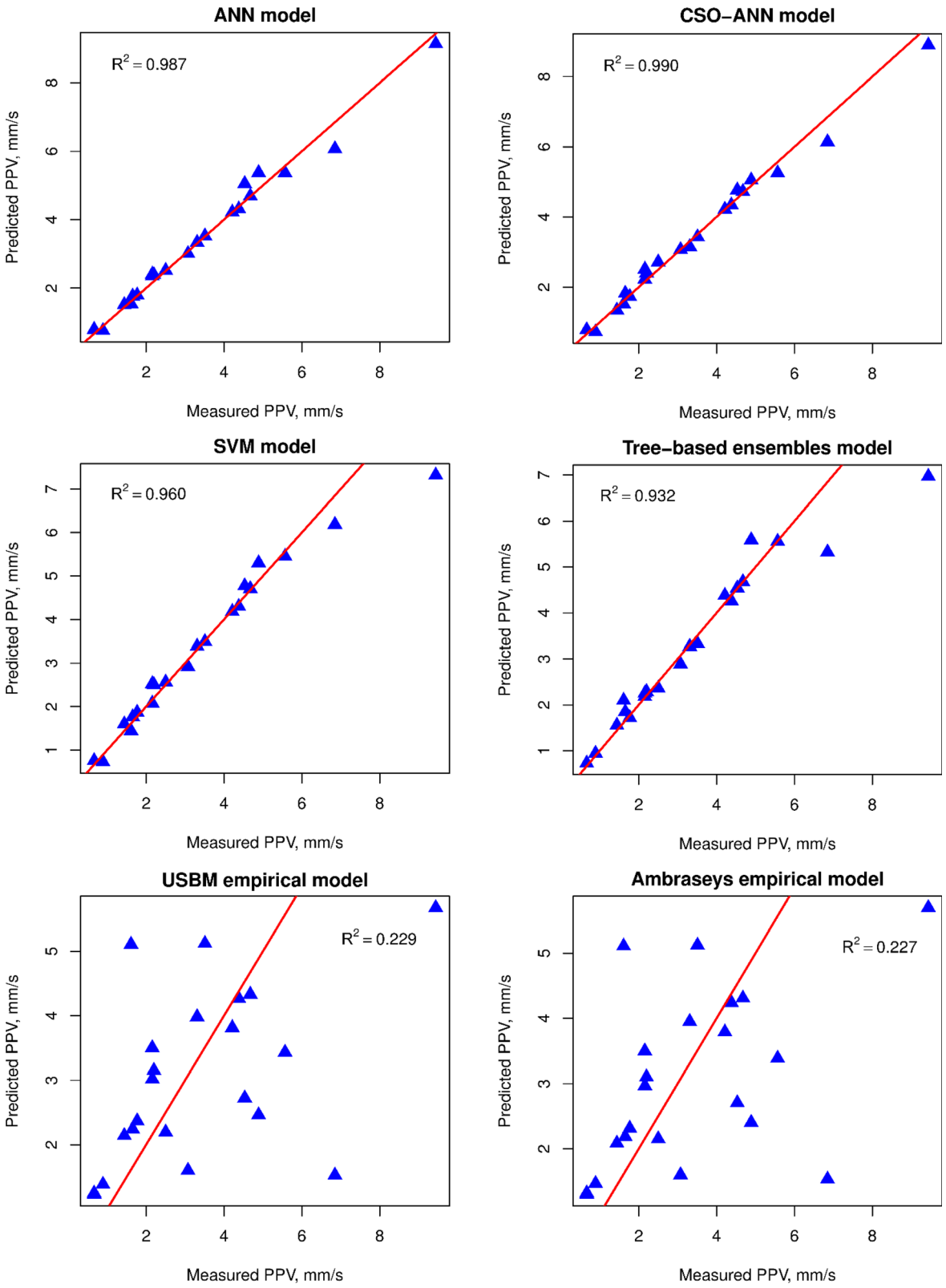
ANN model
$R^2 = 0.987$
Predicted PPV, mm/s
Measured PPV, mm/s
CSO–ANN model
$R^2 = 0.990$
Predicted PPV, mm/s
Measured PPV, mm/s
SVM model
$R^2 = 0.960$
Predicted PPV, mm/s
Measured PPV, mm/s
Tree–based ensembles model
$R^2 = 0.932$
Predicted PPV, mm/s
Measured PPV, mm/s
USBM empirical model
$R^2 = 0.229$
Predicted PPV, mm/s
Measured PPV, mm/s
Ambraseys empirical model
$R^2 = 0.227$
Predicted PPV, mm/s
Measured PPV, mm/s

◀**Figure 11.** Correlation results of the PPV prediction models (testing dataset).

modeled by linear relationships, mostly based on W_{tt} and R only; instead, the AI models can explain the nonlinear relationships of the inputs and output very well, especially the use of multiple (here, 6) input variables. Of the four AI models developed (i.e., ANN, CSO–ANN, SVM, and tree-based ensembles), the tree-based ensembles model provided the lowest accuracy. The accuracy of the SVM was slightly higher than those of the tree-based ensembles model. Considering the ANN model, we can see that it performed better the SVM and tree-based ensembles models in terms of PPV prediction. Remarkably, the CSO-ANN model provided the best performance after optimization by the CSO algorithm. This finding indicated that the CSO algorithm successfully optimized the ANN model, and the accuracy of the ANN model was improved significantly in predicting PPV herein. In other words, the proposed hybrid model, i.e., CSO–ANN, was the model with the most superior performance in this study.

For further assessment of the accuracy and the probability of the developed models, the correlation between measured PPVs and PPVs predicted by the developed models was taken into account (Fig. 11). As depicted in Figure 11, the ANN and CSO predicted ANN models predicted PPV very well with close correspondence between measured and predicted PPVs. However, the ANN model provided a lower accuracy of PPV predictions, especially PPVs in the range of 5–11 mm/s. Similar results were found with the SVM and tree-based ensembles models; however, the regression angle of these models was higher than those of the ANN and CSO–ANN models. They indicated that the reliability of the predictions of these models is quite different from the measured PPVs, even though the correlation coefficient is high. In particular, the empirical models provided incorrect PPVs based on the correlation between measured and predicted PPVs, and on the angle of the regression line in Figure 10. These results are agreement with the computed results given in Table 4. Therefore, the empirical equations should not be used in practical engineering in this mine, even though it is a rapid method for estimation of PPV.

The maximum explosive charge per blast used in this mine is 3000 kg, and many blast patterns were designed with 3000 kg as the total explosive charged. However, the measured PPVs at this site are different because the mine uses the non-electronic delay blasting method, and the delay time of each borehole is different. In addition, the number of boreholes and the other parameters of boreholes are different; therefore, the PPV induced by each blast was not similar or not the same. It is for this reason that we have used the explosive charge per borehole as one of the input variables in this study, and the AI models seem to have exploited this advantage of the dataset used. To further demonstrate this finding, a sensitivity analysis of the input variables was adopted based on the best model (i.e., CSO–ANN model). The sensitivity analysis results are shown in Figure 12. Based on this visualization, we have reason to believe that W_{bh} (maximum explosive charge per borehole) has a significant effect on blast-induced PPV, and it should be used as an essential variable in predicting blast-induced PPV. In addition, the results indicated that R, W_{tt} and W_{bh} were the most critical variables for predicting blast-induced PPV. Of these variables, R has the highest effect on blast-induced PPV, and this is in agreement with the conclusions of Wang et al. (2020). In other previous studies, some researchers stated that PF has a positive effect on blast-induced PPV (e.g., Faradonbeh and Monjezi 2017). However, in this study, PF has a low impact on blast-induced PPV because the hardness of rock mass is not too similar, and the Protodyakonov coefficient (representing hardness of rock mass) was, in this case study, determined to be equal to 12.

VALIDATION OF THE MODELS FOR PRACTICAL ENGINEERING

Once the PPV predictive models were well developed and thoroughly assessed based on both training and testing datasets, their accuracies were verified using three blasts in practical engineering. The data collection steps were similar to the data collection step that was described earlier, and the details of the validation blasting events are listed in Table 5. In addition, the location of blasts and measurement points, as well as the distance between blast sites and seismographs, are depicted in Figure 13. It is worth noting that the seismographs were placed at these locations to record the blast-induced

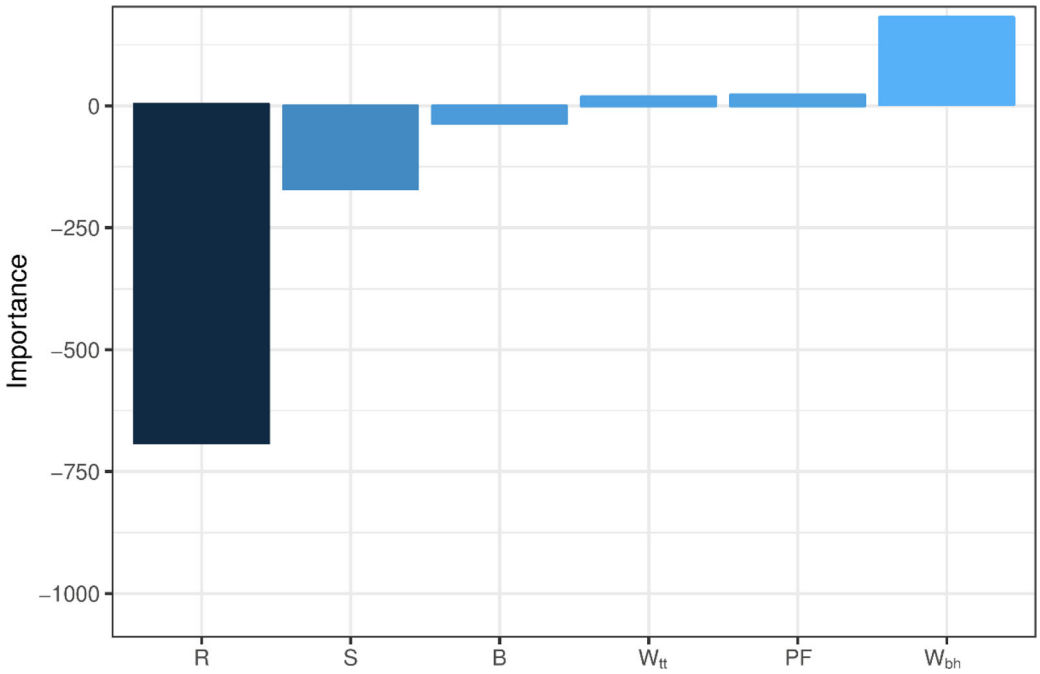

Figure 12. Importance level of the input variables in this study.

Table 5. Validation dataset in practical engineering (3 blasting events)

W_{tt}	W_{bh}	R1	R2	R3	S	B	PF	PPV1	PPV2	PPV3
3000	50	130	125	145	3.3	3.5	0.44	5.563	5.322	5.118
2900	41	125.5	130	223	3.6	3.2	0.45	2.648	2.508	2.386
3000	44	198	203	215	3.4	3.2	0.45	2.912	2.815	2.446

PPV1, PPV2, PPV3 values are corresponding to the R1, R2, R3

PPVs to control the stability of benches and slopes of the mine. Once the input variables were fully collected, they were used to predict PPVs using the developed models. The practical results were then compared with the actual values that were recorded by the seismograph, and the results are listed in Table 6.

From Table 6, we can see that the developed AI models predicted PPVs very well; in particular, the proposed CSO–ANN model predicted PPVs with the highest accuracy. Remarkably, the tree-based ensembles model provided the same accuracy on all three validation blasting events, but its accuracy was the lowest among the AI models developed. This problem occurred because the tree-based ensembles model used the ''mean prediction mode,'' and then all the outcome predictions were computed by their means. The empirical models were still consistent to the results they yielded for the training and testing datasets with considerable deviations, and they do not guarantee the confidence level to predict PPV in this case.

CONCLUSIONS

Ground vibration is an undesirable phenomenon during mine blasting. It decreases the efficiency of blasting operations and it generates many adverse side effects, such as vibration of building, crashing the structure of buildings, instability of benches and slopes, and threatens the lives of workers, as well as breakdown of equipment if landslides occur. Therefore, accurate prediction of

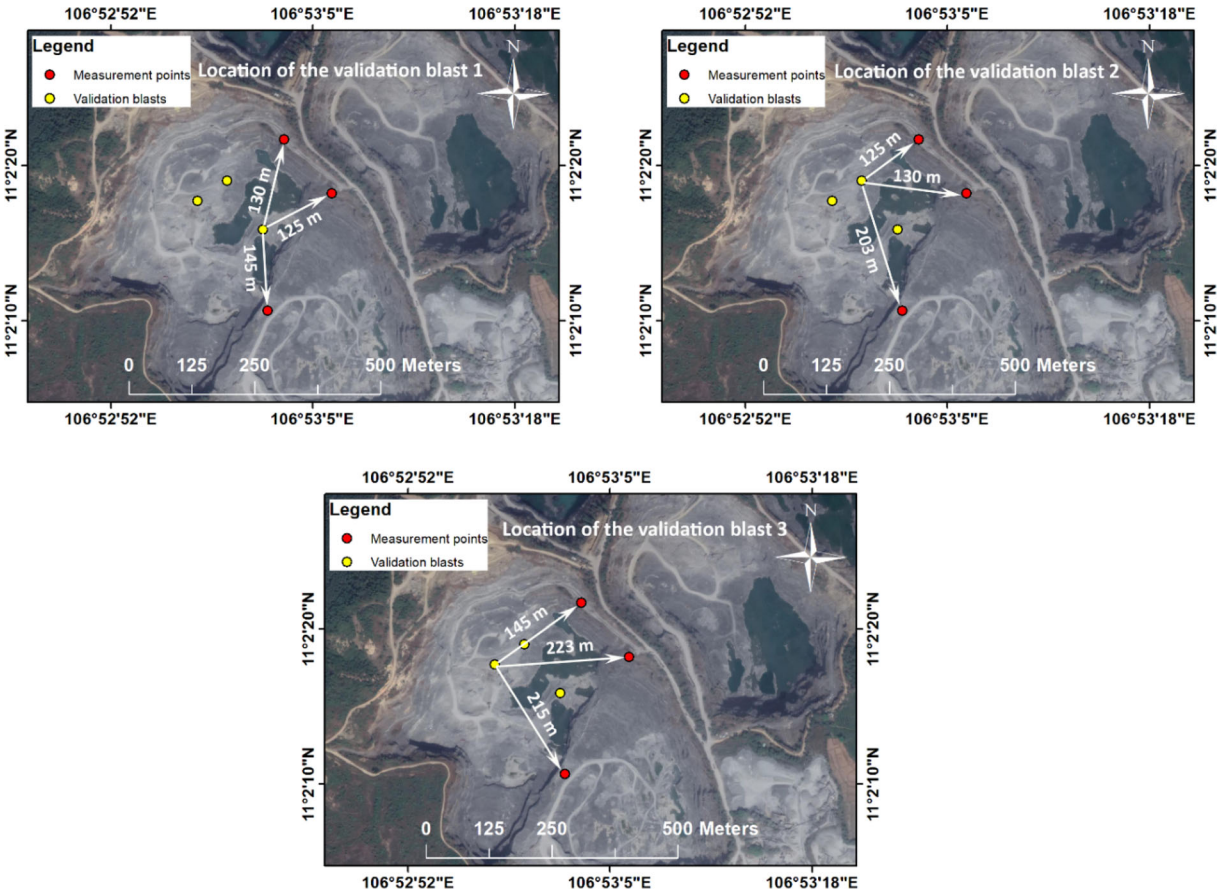

Figure 13. Location of the validation blasts and their monitoring distances.

PPV is crucial to optimize blasting events and to control its undesirable effects. Based on the obtained results, the following conclusions are made.

(1) The AI models are state-of-the-art tools for predicting PPV with high performance. Of those used in this study, the proposed CSO-ANN model is a robust AI model that can be used in PPV prediction, which can help in reduction of the adverse effects of ground vibration.

(2) The CSO algorithm played a vital role in the optimization and enhancement of the ANN model for predicting PPV. AI models should be enhanced and improved by the optimization/metaheuristic algorithms to get better performance and accuracy in practical engineering.

(3) The explosive charge per borehole is an essential parameter in blasting, especially for the electric/non-electric delay blasting methods. In the case of the use of the electric/non-electric delay blasting methods for each borehole, it should be used as the primary parameter to predict blast-induced ground vibration instead of the total explosive charge per blast or maximum explosive charge per row.

(4) Monitoring distance, mass explosive per hole, and total explosive charge per blast are the most important parameters for PPV prediction in mine blasting with high efficiency. For the empirical models, mass explosive per hole, total explosive charge per blast, and maximum explosive charge per row should be taken into account and selected depending on the blasting methods applied. In addition, empirical equations that can explain the nonlinear relationships of the relevant blasting parameters are necessary for future research aiming to improve the accuracy of the inherent empirical equations.

(5) Based on the obtained results, the proposed CSO–ANN model can be used to control, predict, as well as mitigate blast-induced ground vibration in

Table 6. Predictions of the developed models in practical engineering cross-validation

Validation blast	Locations	Measured	ANN	CSO-ANN	SVM	Tree-based ensembles	USBM empirical	Ambraseys empirical
Validation blast 1	Location 1	5.563	5.116	5.329	4.872	4.216	11.674	12.005
	Location 2	5.322	4.952	5.037	4.960	4.216	12.363	12.737
	Location 3	5.118	4.774	4.915	4.642	4.216	9.953	10.180
Validation blast 2	Location 1	2.648	2.471	2.536	3.105	2.088	11.99	12.446
	Location 2	2.508	2.207	2.311	3.016	2.088	11.389	11.802
	Location 3	2.386	2.641	2.505	2.100	2.088	5.177	5.225
Validation blast 3	Location 1	2.912	3.112	3.127	2.798	2.414	6.314	5.616
	Location 2	2.815	2.915	2.911	2.765	2.414	6.088	6.125
	Location 3	2.446	2.236	2.284	2.697	2.414	5.598	5.6160

practical blasting with high reliability. Although the accuracy of this model is ideal in this study, it would be greater if the geological conditions were considered. Future studies may benefit from blasting parameters and geological conditions for more comprehensive assessment and application conditions.

REFERENCES

Abbas, A. S., & Asheghi, R. (2018). Optimised developed artificial neural network-based models to predict the blast-induced ground vibration. *Innovative Infrastructure Solutions, 3,* 1–10.

Abolfathi, S., Yeganeh-Bakhtiary, A., Hamze-Ziabari, S., & Borzooei, S. (2016). Wave runup prediction using M5′ model tree algorithm. *Ocean Engineering, 112,* 76–81.

Afeni, T. B., & Osasan, S. K. (2009). Assessment of noise and ground vibration induced during blasting operations in an open pit mine—A case study on Ewekoro limestone quarry, Nigeria. *Mining Science and Technology (China), 19*(4), 420–424.

Ak, H., Iphar, M., Yavuz, M., & Konuk, A. (2009). Evaluation of ground vibration effect of blasting operations in a magnesite mine. *Soil Dynamics and Earthquake Engineering, 29*(4), 669–676.

Aljarah, I., Faris, H., & Mirjalili, S. (2018). Optimising connection weights in neural networks using the whale optimisation algorithm. *Soft Computing, 22*(1), 1–15.

Ambraseys, N. (1968). Rock mechanics in engineering practice.

Amiri, M., Amnieh, H. B., Hasanipanah, M., & Khanli, L. M. (2016). A new combination of artificial neural network and K-nearest neighbors models to predict blast-induced ground vibration and air-overpressure. *Engineering with Computers, 32*(4), 631–644.

Armaghani, D. J., Hasanipanah, M., Amnieh, H. B., & Mohamad, E. T. (2018). Feasibility of ICA in approximating ground vibration resulting from mine blasting. *Neural Computing and Applications, 29*(9), 457–465.

Armaghani, D. J., Momeni, E., Abad, S. V. A. N. K., & Khandelwal, M. (2015). Feasibility of ANFIS model for prediction of ground vibrations resulting from quarry blasting. *Environmental Earth Sciences, 74*(4), 2845–2860.

Ayaz, Y., Kocamaz, A. F., & Karakoç, M. B. (2015). Modeling of compressive strength and UPV of high-volume mineral-admixtured concrete using rule-based M5 rule and tree model M5P classifiers. *Construction and Building Materials, 94,* 235–240.

Azimi, Y., Khoshrou, S. H., & Osanloo, M. (2019). Prediction of blast induced ground vibration (BIGV) of quarry mining using hybrid genetic algorithm optimised artificial neural network. *Measurement, 147,* 106874.

Bayat, P., Monjezi, M., Rezakhah, M., & Armaghani, D. J. (2020). Artificial neural network and firefly algorithm for estimation and minimisation of ground vibration induced by blasting in a mine. *Natural Resources Research, 29,* 4121–4132.

Besler, E., Wang, Y. C., & Sahakian, A. V. (2019). Real-time Radiofrequency ablation lesion depth estimation using multi-frequency impedance with a deep neural network and tree-based ensembles. *IEEE Transactions on Biomedical Engineering, 67,* 1890–1899.

Borisov, A., Eruhimov, V., & Tuv, E. (2006). Tree-based ensembles with dynamic soft feature selection. *Feature extraction* (pp. 359–374). New York: Springer.

Bui, X.-N., Jaroonpattanapong, P., Nguyen, H., Tran, Q.-H., & Long, N. Q. (2019). A novel Hybrid Model for predicting Blast-induced Ground Vibration Based on k-nearest neighbors and particle Swarm optimisation. *Scientific Reports, 9*(1), 1–14.

Can, A., Dagdelenler, G., Ercanoglu, M., & Sonmez, H. (2019). Landslide susceptibility mapping at Ovacık-Karabük (Turkey) using different artificial neural network models: comparison of training algorithms. *Bulletin of Engineering Geology and the Environment, 78*(1), 89–102.

Chen, W., Hasanipanah, M., Rad, H. N., Armaghani, D. J., & Tahir, M. (2019). A new design of evolutionary hybrid optimisation of SVR model in predicting the blast-induced ground vibration. *Engineering with Computers*, 1–17.

Daniel, G. G. (2013). Artificial Neural Network. In A. L. C. Runehov & L. Oviedo (Eds.), *Encyclopedia of sciences and religions* (pp. 143–143). Dordrecht: Springer.

Dindarloo, S. R. (2015). Prediction of blast-induced ground vibrations via genetic programming. *International Journal of Mining Science and Technology, 25*(6), 1011–1015.

Ding, Z., Nguyen, H., Bui, X.-N., Zhou, J., & Moayedi, H. (2019). Computational intelligence model for estimating intensity of blast-induced ground vibration in a mine based on imperialist competitive and extreme gradient boosting algorithms. *Natural Resources Research*. https://doi.org/10.1007/s11053-019-09548-8.

Duvall, W. I., & Fogelson, D. E. (1962). *Review of criteria for estimating damage to residences from blasting vibrations*: US Department of the Interior, Bureau of Mines.

Efthymiou, A., Barmpounakis, E. N., Efthymiou, D., & Vlahogianni, E. I. (2019). Transportation mode detection from low-power smartphone sensors using tree-based ensembles. *Journal of Big Data Analytics in Transportation, 1*(1), 57–69.

Ekanayake, S. D., Liyanapathirana, D., & Leo, C. J. (2014). Attenuation of ground vibrations using in-filled wave barriers. *Soil Dynamics and Earthquake Engineering, 67,* 290–300.

Fang, Q., Nguyen, H., Bui, X.-N., & Nguyen-Thoi, T. (2019). Prediction of blast-induced ground vibration in open-pit mines using a new technique based on imperialist competitive algorithm and M5Rules. *Natural Resources Research, 29*(2), 791–806.

Faradonbeh, R. S., & Monjezi, M. (2017). Prediction and minimisation of blast-induced ground vibration using two robust meta-heuristic algorithms. *Engineering with Computers, 33*(4), 835–851.

Feng, F., Zhang, C., Ma, J., & Zhang, Q.-J. (2015). Parametric modeling of EM behavior of microwave components using combined neural networks and pole-residue-based transfer functions. *IEEE Transactions on Microwave Theory and Techniques, 64*(1), 60–77.

Fisne, A., Kuzu, C., & Hüdaverdi, T. (2011). Prediction of environmental impacts of quarry blasting operation using fuzzy logic. *Environmental Monitoring and Assessment, 174*(1–4), 461–470.

Gandomi, A. H., Yang, X.-S., & Alavi, A. H. (2013). Cuckoo search algorithm: A metaheuristic approach to solve structural optimisation problems. *Engineering with Computers, 29*(1), 17–35.

Gholami, R., & Fakhari, N. (2017). Support vector machine: principles, parameters, and applications. *Handbook of neural computation* (pp. 515–535). Amsterdam: Elsevier.

Ghoraba, S., Monjezi, M., Talebi, N., Armaghani, D. J., & Moghaddam, M. (2016). Estimation of ground vibration produced by blasting operations through intelligent and empirical models. *Environmental earth sciences, 75*(15), 1137.

Hajihassani, M., Armaghani, D. J., Marto, A., & Mohamad, E. T. (2015a). Ground vibration prediction in quarry blasting through an artificial neural network optimised by imperialist competitive algorithm. *Bulletin of Engineering Geology and the Environment, 74*(3), 873–886.

Hajihassani, M., Armaghani, D. J., Monjezi, M., Mohamad, E. T., & Marto, A. (2015b). Blast-induced air and ground vibration prediction: A particle swarm optimisation-based artificial neural network approach. *Environmental Earth Sciences, 74*(4), 2799–2817.

Hasanipanah, M., Bakhshandeh Amnieh, H., Khamesi, H., Jahed Armaghani, D., Bagheri Golzar, S., & Shahnazar, A. (2018). Prediction of an environmental issue of mine blasting: an imperialistic competitive algorithm-based fuzzy system. *International Journal of Environmental Science and Technology, 15*(3), 551–560.

Hasanipanah, M., Faradonbeh, R. S., Amnieh, H., Armaghani, D., & Monjezi, M. (2017a). Forecasting blast-induced ground vibration developing a CART model. *Engineering with Computers, 33*(2), 307–316.

Hasanipanah, M., Golzar, S. B., Larki, I. A., Maryaki, M. Y., & Ghahremanians, T. (2017b). Estimation of blast-induced ground vibration through a soft computing framework. *Engineering with Computers, 33*(4), 951–959.

Hasanipanah, M., Monjezi, M., Shahnazar, A., Armaghani, D. J., & Farazmand, A. (2015). Feasibility of indirect determination of blast induced ground vibration based on support vector machine. *Measurement, 75,* 289–297.

Hasanipanah, M., Naderi, R., Kashir, J., Noorani, S. A., & Qaleh, A. Z. A. (2017c). Prediction of blast-produced ground vibration using particle swarm optimisation. *Engineering with Computers, 33*(2), 173–179.

Hearst, M. A., Dumais, S. T., Osuna, E., Platt, J., & Scholkopf, B. (1998). Support vector machines. *IEEE Intelligent Systems and their applications, 13*(4), 18–28.

Hosseini, S. A., Tavana, A., Abdolahi, S. M., & Darvishmaslak, S. (2019). Prediction of blast-induced ground vibrations in quarry sites: A comparison of GP, RSM and MARS. *Soil Dynamics and Earthquake Engineering, 119,* 118–129.

Huang, L., Li, J., Hao, H., & Li, X. (2018). Micro-seismic event detection and location in underground mines by using Convolutional Neural Networks (CNN) and deep learning. *Tunnelling and Underground Space Technology, 81,* 265–276.

Hudaverdi, T. (2012). Application of multivariate analysis for prediction of blast-induced ground vibrations. *Soil Dynamics and Earthquake Engineering, 43,* 300–308.

Jafarian, F., Taghipour, M., & Amirabadi, H. (2013). Application of artificial neural network and optimisation algorithms for optimising surface roughness, tool life and cutting forces in turning operation. *Journal of Mechanical Science and Technology, 27*(5), 1469–1477.

Joshi, A. V. (2020). Support vector machines. *Machine learning and artificial intelligence* (pp. 65–71). New York: Springer.

Kaveh, A., Bakhshpoori, T., & Hamze-Ziabari, S. (2016). Derivation of new equations for prediction of principal ground-motion parameters using M5′ algorithm. *Journal of Earthquake Engineering, 20*(6), 910–930.

Kaydani, H., & Mohebbi, A. (2013). A comparison study of using optimisation algorithms and artificial neural networks for predicting permeability. *Journal of Petroleum Science and Engineering, 112,* 17–23.

Khandelwal, M., Kankar, P., & Harsha, S. (2010). Evaluation and prediction of blast induced ground vibration using support vector machine. *Mining Science and Technology (China), 20*(1), 64–70.

Khandelwal, M., Kumar, D. L., & Yellishetty, M. (2011). Application of soft computing to predict blast-induced ground vibration. *Engineering with Computers, 27*(2), 117–125.

Kumar, S., & Mishra, A. K. (2020). Reduction of blast-induced ground vibration and utilisation of explosive energy using low-density explosives for environmentally sensitive areas. *Arabian Journal of Geosciences, 13*(14), 1–10.

Leardi, R. (2003). *Nature-inspired methods in chemometrics: Genetic algorithms and artificial neural networks*. Amsterdam: Elsevier.

Ma, Y., & Guo, G. (2014). *Support vector machines applications*. New York: Springer.

Mareli, M., & Twala, B. (2018). An adaptive Cuckoo search algorithm for optimisation. *Applied Computing and Informatics, 14*(2), 107–115.

Mirjalili, S., Hashim, S. Z. M., & Sardroudi, H. M. (2012). Training feedforward neural networks using hybrid particle swarm optimisation and gravitational search algorithm. *Applied Mathematics and Computation, 218*(22), 11125–11137.

Mohamadnejad, M., Gholami, R., & Ataei, M. (2012). Comparison of intelligence science techniques and empirical methods for prediction of blasting vibrations. *Tunnelling and Underground Space Technology, 28,* 238–244.

Mokfi, T., Shahnazar, A., Bakhshayeshi, I., Derakhsh, A. M., & Tabrizi, O. (2018). Proposing of a new soft computing-based model to predict peak particle velocity induced by blasting. *Engineering with Computers, 34,* 881–888.

Monjezi, M., Ahmadi, M., Sheikhan, M., Bahrami, A., & Salimi, A. (2010). Predicting blast-induced ground vibration using various types of neural networks. *Soil Dynamics and Earthquake Engineering, 30*(11), 1233–1236.

Monjezi, M., Baghestani, M., Faradonbeh, R. S., Saghand, M. P., & Armaghani, D. J. (2016). Modification and prediction of blast-induced ground vibrations based on both empirical and

computational techniques. *Engineering with Computers, 32*(4), 717–728.
Monjezi, M., Hasanipanah, M., & Khandelwal, M. (2013). Evaluation and prediction of blast-induced ground vibration at Shur River Dam, Iran, by artificial neural network. *Neural Computing and Applications, 22*(7–8), 1637–1643.
Murlidhar, B. R., Armaghani, D. J., & Mohamad, E. T. (2020). Intelligence prediction of some selected environmental issues of blasting: A review. *The Open Construction & Building Technology Journal, 14*(1), 298–308.
Nerguizian, C., Despins, C., & Affès, S. (2006). Geolocation in mines with an impulse response fingerprinting technique and neural networks. *IEEE Transactions on Wireless Communications, 5*(3), 603–611.
Nguyen, H., & Bui, X.-N. (2019). Predicting blast-induced air overpressure: A robust artificial intelligence system based on artificial neural networks and random forest. *Natural Resources Research, 28*(3), 893–907.
Nguyen, H., Bui, X.-N., Bui, H.-B., & Cuong, D. T. (2019a). Developing an XGBoost model to predict blast-induced peak particle velocity in an open-pit mine: A case study. *Acta Geophysica, 67*(2), 477–490.
Nguyen, H., Bui, X.-N., Tran, Q.-H., & Mai, N.-L. (2019b). A new soft computing model for estimating and controlling blast-produced ground vibration based on hierarchical K-means clustering and cubist algorithms. *Applied Soft Computing, 77,* 376–386.
Nguyen, H., Bui, X.-N., Tran, Q.-H., & Moayedi, H. (2019c). Predicting blast-induced peak particle velocity using BGAMs, ANN and SVM: A case study at the Nui Beo open-pit coal mine in Vietnam. *Environmental earth sciences, 78*(15), 479.
Nguyen, H., Choi, Y., Bui, X.-N., & Nguyen-Thoi, T. (2019d). Predicting blast-induced ground vibration in open-pit mines using vibration sensors and support vector regression-based optimisation algorithms. *Sensors, 20*(1), 132.
Nguyen, H., Drebenstedt, C., Bui, X.-N., & Bui, D. T. (2019e). Prediction of blast-induced ground vibration in an open-pit mine by a novel hybrid model based on clustering and artificial neural network. *Natural Resources Research, 29*(2), 691–709.
Nguyen, H., Moayedi, H., Jusoh, W. A. W., & Sharifi, A. (2019f). Proposing a novel predictive technique using M5Rules-PSO model estimating cooling load in energy-efficient building system. *Engineering with Computers*. https://doi.org/10.1007/s00366-019-00735-y.
Nguyen, N. T. T., & Tong, H. T. (2020). Predicting land use change base on GIS and remote sensing. *Journal of Mining and Earth Sciences*, *61*(2), 106–115.
Nguyen, A. D., Tran, H. Q., Tran, B. D., & Soukhanouvong, P. (2020). Prediction of the peak velocity of blasting vibration based on various models at Ninh Dan quarry, Thanh Ba district, Phu Tho province. *Journal of Mining and Earth Sciences*, *61*(4), 102–109.
Oliveira, R., Camanho, A. S., & Zanella, A. (2017). Expanded eco-efficiency assessment of large mining firms. *Journal of Cleaner Production, 142,* 2364–2373.
Prasad, R., Pandey, A., Singh, K., Singh, V., Mishra, R., & Singh, D. (2012). Retrieval of spinach crop parameters by microwave remote sensing with back propagation artificial neural networks: A comparison of different transfer functions. *Advances in Space Research, 50*(3), 363–370.
Raina, A., Chakraborty, A., Choudhury, P., & Sinha, A. (2011). Flyrock danger zone demarcation in opencast mines: A risk based approach. *Bulletin of Engineering Geology and the Environment, 70*(1), 163–172.
Rezaei, M., Monjezi, M., & Varjani, A. Y. (2011). Development of a fuzzy model to predict flyrock in surface mining. *Safety Science, 49*(2), 298–305.
Saadat, M., Khandelwal, M., & Monjezi, M. (2014). An ANN-based approach to predict blast-induced ground vibration of Gol-E-Gohar iron ore mine, Iran. *Journal of Rock Mechanics and Geotechnical Engineering, 6*(1), 67–76.
Samareh, H., Khoshrou, S. H., Shahriar, K., Ebadzadeh, M. M., & Eslami, M. (2017). Optimisation of a nonlinear model for predicting the ground vibration using the combinational particle swarm optimisation-genetic algorithm. *Journal of African Earth Sciences, 133,* 36–45.
Shahnazar, A., Rad, H. N., Hasanipanah, M., Tahir, M., Armaghani, D. J., & Ghoroqi, M. (2017). A new developed approach for the prediction of ground vibration using a hybrid PSO-optimized ANFIS-based model. *Environmental Earth Sciences, 76*(15), 527.
Shang, Y., Nguyen, H., Bui, X.-N., Tran, Q.-H., & Moayedi, H. (2019). A novel artificial intelligence approach to predict blast-induced ground vibration in open-pit mines based on the firefly algorithm and artificial neural network. *Natural Resources Research, 29*(2), 723–737.
Sheykhi, H., Bagherpour, R., Ghasemi, E., & Kalhori, H. (2018). Forecasting ground vibration due to rock blasting: A hybrid intelligent approach using support vector regression and fuzzy C-means clustering. *Engineering with Computers, 34*(2), 357–365.
Singh, T., & Singh, V. (2005). An intelligent approach to prediction and control ground vibration in mines. *Geotechnical & Geological Engineering, 23*(3), 249–262.
Taheri, K., Hasanipanah, M., Golzar, S. B., & Majid, M. Z. A. (2017). A hybrid artificial bee colony algorithm-artificial neural network for forecasting the blast-produced ground vibration. *Engineering with Computers, 33*(3), 689–700.
Tran, V. T. T. (2020). Dynamic symbol for electronic map, network map and the ability to create dynamic symbol on the map with the online answering machine. *Journal of Mining and Earth Sciences, 61*(3), 88–98.
Tran, T. M., Do, T. N., Dinh, H. T. T., Vu, H. X., & Ferrier, E. (2020). A 2-D numerical model of the mechanical behavior of the textile-reinforced concrete composite material: effect of textile reinforcement ratio. *Journal of Mining and Earth Sciences*, *61*(3), 51–59.
Tripathy, G., & Gupta, I. (2002). Prediction of ground vibrations due to construction blasts in different types of rock. *Rock Mechanics and Rock Engineering, 35*(3), 195–204.
Verma, A., & Singh, T. (2011). Intelligent systems for ground vibration measurement: A comparative study. *Engineering with Computers, 27*(3), 225–233.
Vu, Q. T., Pham, M. N., Dang, C. M., Vuong, H. H., Duong, H. D., Bui, T. T., et al. (2020) Fuzzy logic in controlling the forest fire-level forecast warning signage. *Journal of Mining and Earth Sciences*, *61*(4), 126–136.
Wang, G.-G., Gandomi, A. H., Zhao, X., & Chu, H. C. E. (2016). Hybridising harmony search algorithm with cuckoo search for global numerical optimisation. *Soft Computing, 20*(1), 273–285.
Wang, K., Liu, Z., Qian, X., & He, Y. (2020). Dynamic characteristics and damage recognition of blast-induced ground vibration for natural gas transmission pipeline and its integrated systems. *Mechanical Systems and Signal Processing, 136,* 106472.
Xue, X. (2019). Neuro-fuzzy based approach for prediction of blast-induced ground vibration. *Applied Acoustics, 152,* 73–78.
Yan, Y., Hou, X., & Fei, H. (2020). Review of predicting the blast-induced ground vibrations to reduce impacts on ambient urban communities. *Journal of cleaner production, 260,* 121135.
Yang, H., Hasanipanah, M., Tahir, M. M., & Bui, D. T. (2019). Intelligent prediction of blasting-induced ground vibration

using ANFIS optimised by GA and PSO. *Natural Resources Research, 29*(2), 739–750.

Yang, X.-S., & Deb, S. (2009). Cuckoo search via Lévy flights. In: *2009 World congress on nature & biologically inspired computing (NaBIC)* (pp. 210–214). IEEE.

Yang, X.-S., & Deb, S. (2014). Cuckoo search: recent advances and applications. *Neural Computing and Applications, 24*(1), 169–174.

Ye, H., Liang, L., Li, G. Y., & Juang, B.-H. (2020). Deep learning-based end-to-end wireless communication systems with conditional GANs as unknown channels. *IEEE Transactions on Wireless Communications, 19*(5), 3133–3143.

Yu, Z., Shi, X., Zhou, J., Chen, X., & Qiu, X. (2020a). Effective assessment of blast-induced ground vibration using an optimised random forest model based on a Harris Hawks optimization algorithm. *Applied Sciences, 10*(4), 1403.

Yu, Z., Shi, X., Zhou, J., Gou, Y., Huo, X., Zhang, J., et al. (2020b). A new multikernel relevance vector machine based on the HPSOGWO algorithm for predicting and controlling blast-induced ground vibration. *Engineering with Computers*, 1–16.

Zăvoianu, A.-C., Bramerdorfer, G., Lughofer, E., Silber, S., Amrhein, W., & Klement, E. P. (2013). Hybridisation of multi-objective evolutionary algorithms and artificial neural networks for optimising the performance of electrical drives. *Engineering Applications of Artificial Intelligence, 26*(8), 1781–1794.

Zgür Akkoyun, Ö., & Taskıran, T. . (2015). Investigation of blast-induced ground vibration effects on rural buildings. *Structural Engineering and Mechanics, 54*(3), 545–560.

Zhang, X., Nguyen, H., Bui, X.-N., Tran, Q.-H., Nguyen, D.-A., Bui, D. T., et al. (2019). Novel soft computing model for predicting blast-induced ground vibration in open-pit mines based on particle swarm optimization and XGBoost. *Natural Resources Research, 29*(2), 711–721.

Zhou, J., Asteris, P. G., Armaghani, D. J., & Pham, B. T. (2020). Prediction of ground vibration induced by blasting operations through the use of the Bayesian Network and random forest models. *Soil Dynamics and Earthquake Engineering, 139,* 106390.

Zou, J., Han, Y., & So, S.-S. (2008). Overview of artificial neural networks. *Artificial neural networks* (pp. 14–22). New York: Springer.